



**INDC(NDS)-0888**  
**Distr. MP,ST,G**

# **INDC International Nuclear Data Committee**

## **NEUTRON DATA STANDARDS**

Summary Report of the IAEA Technical Meeting

IAEA Headquarters, Vienna, Austria  
9 – 13 October 2023

G. Noguere  
CEA/DES/IRESNE/DER/SPRC/LEPh  
Cadarache, France

D. Neudecker  
Los Alamos National Laboratory  
Los Alamos, NM, USA

G. Schnabel  
International Atomic Energy Agency  
Vienna, Austria

January 2025

---

**IAEA Nuclear Data Section**  
**Vienna International Centre, P.O. Box 100, 1400 Vienna, Austria**

---

INDC documents may be downloaded in electronic form from  
<http://nds.iaea.org/publications>.  
Requests for hardcopy or e-mail transmittal should be directed to

[NDS.Contact-Point@iaea.org](mailto:NDS.Contact-Point@iaea.org)

or to:

Nuclear Data Section  
International Atomic Energy Agency  
Vienna International Centre  
PO Box 100  
1400 Vienna  
Austria

## NEUTRON DATA STANDARDS

### Summary Report of the IAEA Technical Meeting

IAEA Headquarters, Vienna, Austria  
9 – 13 October 2023

G. Noguere  
CEA/DES/IRESNE/DER/SPRC/LEPh  
Cadarache, France

D. Neudecker  
Los Alamos National Laboratory  
Los Alamos, NM, USA

G. Schnabel  
International Atomic Energy Agency  
Vienna, Austria

#### ABSTRACT

A Technical Meeting on Neutron Data Standards was held from 9 to 13 October 2023 with the objective to review recent work and facilitate the coordination of work towards the next release of the Neutron Data Standards. The topics discussed included the review of data of recent experimental campaigns, ongoing evaluation work, the proposal of cross section integrals as references, improvements of evaluation methodology as well as ongoing code developments. 21 participants from eight Member States took part in the meeting. A list of recommendations and actions was issued to coordinate the next steps.

January 2025



## Contents

1.	INTRODUCTION.....	1
2.	TOPICS ADRESSED DURING THE MEETING .....	1
2.1.	Light elements .....	1
2.2.	Fission cross section of $^{235}\text{U}$ .....	3
2.3.	Fission cross section of $^{239}\text{Pu}$ .....	4
2.4.	Prompt fission neutron spectrum .....	4
2.5.	Spectrum average cross section.....	4
2.6.	Thermal neutron constants .....	5
2.7.	Codes and evaluation methods.....	5
2.8.	Review of the GMA database .....	6
3.	PRESENTATION SUMMARIES.....	6
3.1.	The hydrogen standards – The first and uniquely so, A.D. Carlson (NIST, USA) .....	6
3.2.	Progress on the development of gmapy, G. Schnabel (IAEA, Vienna) .....	7
3.3.	Progress on the validation of the Thermal Neutron Constants, G. Noguere (CEA, France)....	8
3.4.	NIFFTE fissionTPC status update on $^{239}\text{Pu}(n,f)/^{235}\text{U}(n,f)$ and $^{235}\text{U}(n,f)/^6\text{Li}(n,f)$ cross section ratio measurements, M. Anastasiou, L. Snyder (LLNL, USA) .....	9
3.5.	New integral references for fissile actinides, I. Duran (USC, Spain).....	10
3.6.	Ratios of the cross sections for the $^{10}\text{B}(n,\alpha)^7\text{Li}$ reaction to the $^6\text{Li}(n,t)^4\text{He}$ reaction, J. Liu (Peking University, China).....	16
3.7.	Measurement of the fission cross-section of $^{235}\text{U}$ relative to n-p scattering from 10 to 70 MeV at CSNS Back-n, Y. Chen (IHEP/CAS, China) .....	17
3.8.	Absolute cross section of the $^{235}\text{U}(n,f)$ in the energy range between 20 and 450 MeV at CERN n_TOF, A. Manna (UNIBO, Italy) .....	17
3.9.	Angular distribution measurements of neutron elastic scattering by natural carbon at GELINA with the ELISA setup, G. Noguere (CEA, France) .....	19
3.10.	A comparison of Gaussian process regression with GLS results for $^{235}\text{U}(n,f)$ cross section, H. Iwamoto (JAEA, Japan).....	19
3.11.	Impact and utility of SACS, R. Capote (IAEA) .....	19
3.12.	Spectrum related SACS uncertainties, D. Smith .....	20
3.13.	$^{235}\text{U}$ and $^{238}\text{U}$ capture at thermal and sub thermal neutron energies, A. Wallner (HZDR, Germany) .....	21
3.14.	AIACHNE work towards a new $^{252}\text{Cf}(sf)$ PFNS evaluation, D. Neudecker (LANL, USA) .....	21
3.15.	Bias identification in nuclear data measurements for experiment design, D. Neudecker (LANL, USA) .....	22
3.16.	New experimental data for the GMAPy database update since 2017 evaluation, V.G. Pronyaev (private, Russia) .....	23
3.17.	Evaluations for $^1\text{H}$ , $^3\text{He}(n,p)$ , $^7\text{Li}$ , $^{11}\text{B}$ , $^{13}\text{C}$ systems with RAC, Z. Chen (Tsinghua University, China).....	28
3.18.	Recent light-element standards-related work at Los Alamos, G. Hale, M. Paris, H. Sasaki (LANL, USA).....	29
4.	REVIEW OF RECOMMENDATIONS AND ACTIONS OF PREVIOUS MEETING.....	30
5.	RECOMMENDATIONS AND ACTIONS.....	30
	APPENDIX I: ADOPTED AGENDA .....	33
	APPENDIX II: PARTICIPANTS.....	35



## 1. INTRODUCTION

Roberto Capote, co-host of the meeting, welcomed all participants and elaborated on essential topics that need to be addressed within this meeting in order to determine necessary activities for the preparation of the next release of the Standards, such as the consideration of SACS measurements as an ingredient in the Standards evaluation process and the treatment of Unrecognized Sources of Uncertainty (USU). He also stressed the role and dependence of the neutron standard evaluation on R-matrix models for light elements and the importance of non-model evaluations for fission and capture cross sections using new experimental data.

Georg Schnabel, who served as the IAEA meeting host, briefly went through the proposed agenda. Allan Carlson was appointed Chair of the meeting and Gilles Noguere agreed to act as rapporteur.

The hybrid meeting took place 9-13 October 2023 and was attended by 21 participants (7 in-person, 14 remote) from eight member states and one international organization, plus IAEA staff, with daily convening times 2pm to 6pm CET. The adopted agenda can be found in Appendix I, the participants' list in Appendix II and links to participants' presentations in Appendix III.

## 2. TOPICS ADRESSED DURING THE MEETING

Works presented during the meeting can be divided into 8 items. Six of them deal with light elements,  $^{235}\text{U}$ ,  $^{239}\text{Pu}$ , PFNS, SACS and TNC and the remaining two items are dedicated to improving codes and the Neutron Standards database.

### 2.1. Light elements

Evaluation activities on light elements were presented by A. Carlson, G. Hale and Z. Chen. Ongoing experimental works were presented by M. Anastasiou and J. Liu.

$^1\text{H}(n,n)$  cross section is a standard (primary standard) below 20 MeV.

Allan Carlson gives a short overview of the history of the hydrogen experimental work. Originally, this activity was connected to the Manhattan project. Two pioneering experimental works have been presented: In the early 1940s, one of the first total scattering cross section measurements of hydrogen was obtained by Bailey from transmission measurements of  $\text{C}_6\text{H}_{12}$  and carbon for neutrons of energies 0.35 to 6.0 MeV. (C.L. Bailey, et al., Phys. Rev. 70 (1946) 583). Combining those data with results by Barschall provided hydrogen scattering angular distributions (SAD). (H.H. Barschall and M.H. Kanner, Phys. Rev. 58 (1940) 590)

#### 2.1.1. Evaluation activities on light elements

The use of theoretical models is a necessity in order to cover missing data as a function of angle and energy (e.g. models based on effective potential, such as the Gammel-Thaler nucleon-nucleon potential). The new evaluation from LANL will be based on a R-Matrix analysis combined possibly with the Arndt phase-shift data using the EDA code. The limit of this approach is about 250 MeV. Note that, if  $^1\text{H}$  measurements are independent of any other cross sections, the evaluation procedure will introduce some correlations with other quantities. Table 1 summarizes ongoing and planned evaluation work performed with the EDA code as well as conclusions derived from an analysis with the RAC code.

TABLE 1. Short review of the evaluation works performed with EDA and RAC (2023).

	EDA	RAC (2023)
<sup>1</sup> H	<ul style="list-style-type: none"> <li>• n-p scattering evaluation up to 250 MeV is in progress.</li> <li>• Charge independent analysis of N-N system up to 100 MeV (various reaction channels are included, 50 free parameters, various types of observables, <math>\chi^2=1.0165</math>).</li> <li>• Extension up to 250 MeV requires more partial waves and background poles (automatic search module of EDA can help to extend the model).</li> <li>• New data added to go up to 250 MeV (pp angular distribution, np angle-integrated cross section, Arndt' NN database).</li> </ul>	<ul style="list-style-type: none"> <li>• n-p scattering evaluation below 1 MeV agrees well with the STD evaluation of 2017.</li> <li>• Above 1 MeV, some structures need to be explained.</li> </ul>
<sup>3</sup> He	<ul style="list-style-type: none"> <li>• n+<sup>3</sup>He evaluation up to 20 MeV was submitted to ENDF/B-VIII.1 (standard up to 50 keV, no change below 200 keV).</li> <li>• Coherence description of the angle-integrated cross section and SAD for <sup>3</sup>He(n,p) and <sup>3</sup>He(n,d).</li> <li>• <sup>3</sup>He(n,<math>\gamma</math>) follow available data.</li> <li>• The evaluation in the standards range hasn't change since ENDF/B-VI</li> </ul>	<ul style="list-style-type: none"> <li>• <sup>3</sup>He(n,p) evaluation agrees with ENDF/B-VII evaluation.</li> </ul>
Li	<ul style="list-style-type: none"> <li>• n+<sup>6</sup>Li still in progress to go up to 8 MeV.</li> <li>• Better data are needed up to at least 5 MeV.</li> </ul>	<ul style="list-style-type: none"> <li>• Various direct and inverse reaction channels are included for the evaluation of the <sup>7</sup>Li system.</li> <li>• Excellent agreement with ENDF/B-VII for the total cross section.</li> <li>• For elastic channel, at lower energy, ENDF/B-VII seems to be too high compared to data and present evaluation.</li> <li>• <sup>6</sup>Li(n,t) is in good agreement with STD, with a difference of about 2% in the wings of the resonance compared to STD.</li> </ul>
B	<ul style="list-style-type: none"> <li>• No new work has been done on the n+<sup>10</sup>B reaction</li> </ul>	<ul style="list-style-type: none"> <li>• Various direct and inverse reaction channels are included for the evaluation of the <sup>11</sup>B system.</li> <li>• Total cross section is in good agreement with ENDF/B-VII.</li> <li>• The elastic channel in ENDF/B-VII is slightly overestimated in the low energy range.</li> <li>• <sup>10</sup>B(n,<math>\alpha</math>) differences of about -2% to + 6% compared to STD.</li> <li>• <sup>10</sup>B(n,<math>\alpha_0</math>) differences above 10 MeV (no data).</li> <li>• <sup>10</sup>B(n,<math>\alpha_1</math>) good agreement.</li> </ul>
C	<ul style="list-style-type: none"> <li>• <sup>13</sup>C system extension up to 8 MeV (various reaction channels are included, <math>\chi^2=1.40</math>).</li> <li>• One of the problems concerns the <sup>12</sup>C(n,n<sub>1</sub>) reaction around 6.3 MeV (differences between the CoGNAC experiment and Negret data while both datasets are derived from (n,n'<math>\gamma</math>) measurements) but this may not impact the standards region.</li> <li>• New measurements reported at this meeting by Noguere indicate higher angular distribution results from 1.2 to 1.8 MeV at 163.8 degrees. This should be taken into account in new evaluations.</li> </ul>	<ul style="list-style-type: none"> <li>• Various direct and inverse reaction channels are included for the evaluation of the <sup>13</sup>C system.</li> <li>• <sup>12</sup>C(n,tot) and <sup>12</sup>C(n,n) in good agreement with STD (for elastic cross section the differences range from -1% to +2%).</li> <li>• New data from Peking University available for <sup>12</sup>C(n,n+3<math>\alpha</math>) below 15 MeV.</li> </ul>

For high energy fission cross-section measurements, there is a need to extend the hydrogen standard up to 1 GeV. If possible, this will require to include pion degrees of freedom in the R-matrix fit (the pion emission threshold is close to 300 MeV).

A short review of the evaluation activities performed with the EDA code (G. Hale, M. Paris) and the RAC (2023) code (Z. Chen) is given in Table 1. RAC can play an active role in the next evaluation of the STD. It was suggested that RAC and EDA share the same database for consistency.

Another problem related to hydrogen is its capture cross section value and its uncertainty at the thermal point. These quantities have a sizeable impact on light water reactor applications. However, the hydrogen capture cross section is not a standard and relevance of this issue for the standards project needs to be assessed.

### 2.1.2. Experimental activities on light elements

Experimental activities on light elements were conducted at the LANL and CSNS Back-n facility.

Maria Anastasiou presented the ongoing data analysis of the  ${}^6\text{Li}(n,t)$  reaction up to 2-3 MeV measured with the TPC setup developed at LANL within the NIFFTE project. Due to the orientation of the  ${}^6\text{Li}$  sample, the measured yield is not usable at angles around  $90^\circ$ . The  ${}^6\text{Li}(n,nt)$  reaction will be also measured. Results are expected to be released end of 2024 or beginning of 2025.

Jie Liu presented a new analysis of previous measurements carried out at the CSNS Back-n facility by Jiang et al. [Jiang et al., Chin. Phys. C 43, 124002, 2019] and Bai et al. [H. Bai et al. Chin. Phys. C 44, 014003, 2020]. Measurements were done separately for  ${}^{10}\text{B}(n,\alpha)$  and  ${}^6\text{Li}(n,t)$  with the same detector, and neutron flux monitor by trying to get the same geometry. The neutron flux has a maximum at around 1 MeV and covers a large neutron energy range. Reaction angular distributions are measured with silicon detectors covering scattering angles ranging from  $19.2^\circ$  to  $160.8^\circ$ . The normalization of the data is performed in the low energy range [1 eV-10 keV] using STD values. The relative uncertainty below 0.5 MeV is very good (lower than 5%). The present re-analysis of the data confirms the latest STD values for Boron and Lithium. It is expected that the EXFOR compilation will contain all information needed to use these data in the standards evaluation procedure. New analysis of these data was done in which ratios of the reactions were obtained so the dependence on fluence was removed (see Liu, J., Bai, H., Jiang, H. et al. Ratios of the cross sections for the  ${}^{10}\text{B}(n,\alpha){}^7\text{Li}$  reaction. Eur. Phys. J. A 59, 106 (2023)). This is reported in the summaries below.

### 2.2. Fission cross section of ${}^{235}\text{U}$

Ignacio Duran highlighted issues in the evaluation of  ${}^{235}\text{U}(n,f)$  cross section above 200 MeV, and especially between 200 and 400 MeV where pion production becomes energetically feasible. The large spread between the data led to different GMA fits in 2015 and 2017 (which have never been distributed online). Theoretical studies performed with INCL+ABLA and experimental campaigns carried out at n\_TOF and CSNS Back-n will help solving these issues.

Yonghao Chen presented measurements performed at the CSNS Back-n facility between 10 and 70 MeV. The CSNS neutron source is running since 2018 (beam power of 140 kW, double bunch mode, tungsten target). A new CSNS-II neutron source will be available in 2029 (beam power of 500 kW). The Back-n facility is a TOF facility with two experimental areas at L=55 m and 76 m (beam diameter of 3 cm or 6 cm, beam profile not yet precisely characterized,  $T_0$  given by  $\gamma$ -fission events induced by  $\gamma$ -flash). The results between 10 and 70 MeV were obtained by combining a fission chamber and a proton recoil telescope. The experiments were designed for  ${}^{232}\text{Th}$  with various  ${}^{235}\text{U}$  targets. Results for  ${}^{235}\text{U}$  relative to  ${}^1\text{H}$  are still preliminary.

Alice Manna presented the  $^{235}\text{U}(n,f)$  measurement relatively to  $^1\text{H}$ , which were performed at n\_TOF (L=185 m) from 10 to 450 MeV. Two fission chambers (PPFC and PPAC) were used, combined to three telescope type detectors for neutron flux measurements using  $\text{C}_2\text{H}_4$  samples. The experimental  $^{235}\text{U}(n,f)$  cross section is in good agreement with Lisowski data (up to 200 MeV). Some differences are observed around 40 MeV (higher value compared to Lisowski) that seem to be confirmed by the data measured at CSNS Back-n facility (see presentation of Y. Chen). The work of Alice Manna confirms that Kotov data are the best dataset above 400 MeV. However, between 200 and 400 MeV, the question is still open. New experimental campaigns are planned for improving statistics and increasing the upper energy limit.

### 2.3. Fission cross section of $^{239}\text{Pu}$

Lucas Snyder presented two measurements of the ratio  $^{239}\text{Pu}(n,f)/^{235}\text{U}(n,f)$  which were performed at LANL in the energy range from 100 keV to 100 MeV with a TPC developed within the NIFFTE project.

The first experimental results released in 2021 are shape data. Therefore, a second experimental campaign was performed with uniform  $^{235}\text{U}$  target (1 cm diameter with the beam diameter slightly larger). Normalization issues are still under investigation. Due to the normalization, above 30 MeV, the present data are in-between Lisowski and Tovesson data. Therefore, it is still difficult to reduce uncertainties above 30 MeV in the GMA analysis.

### 2.4. Prompt fission neutron spectrum

Denise Neudecker presented activities on PFNS (AIACHNE project). The first objective consisted in reviewing 26 datasets for PFNS ( $^{252}\text{Cf}$ ), that were previously lost, as follows:

- Verification of datasets rejected by Mannhart when justifications are documented;
- Inspection of datasets not used by Mannhart without clear justification;
- Add new datasets reported after Mannhart's work;
- Replace datasets by final published values when issues were found between data used by Mannhart and EXFOR data;
- Systematic investigation of biases related to  $^6\text{Li}$  resonance (measurements performed with  $^6\text{Li}$  detector), efficiency, anisotropy of the fission fragment emission.

Roberto Capote reminded that Blain data (2017) should be rejected because of experimental issues (scattering effects). In addition, it is recommended to use Kornilov data for experimental validation because partial uncertainties are not available (the experiment was originally designed to verify Mannhart's evaluation). The final evaluation is not yet ready. Uncertainties on the new evaluation are still preliminary.

### 2.5. Spectrum average cross section

Roberto Capote and Donald Smith presented the status of the SACS data. It is suggested to use SACS data in the GMA analysis. SACS data and uncertainties for many reactions and neutron spectra were evaluated in the framework of IRDF-II (see INDC(NDS)-0864). The SACS data related to  $^{252}\text{Cf}$  will be based on the updated PNFS of Mannhart, which is under investigation within the AIACHNE project. For SACS data related to  $^{235}\text{U}$ , various issues were discussed.

Denise Neudecker indicated that the PFNS( $^{235}\text{U}$ ) quality is rather poor above 10 MeV and the shape at low energy is also questionable because of the limited number of consistent datasets compared to PFNS( $^{252}\text{Cf}$ ). In addition, some PFNS( $^{235}\text{U}$ ) measurements were performed in a less favorable sample environment than those performed with  $^{252}\text{Cf}$  sources (multiple scattering effects, ...). However, it is important to note that SACS data are not so sensitive to the left and right wings of PFNS, and

experimental validation studies demonstrate that PFNS( $^{235}\text{U}$ ) provide results consistent with PFNS( $^{252}\text{Cf}$ ). Indeed, results using PFNS( $^{252}\text{Cf}$ ) and PFNS( $^{235}\text{U}$ ) seem to indicate that standards released in 2017 give C/E results close to 0.98 in average for  $^{239}\text{Pu}(n,f)/^{235}\text{U}(n,f)$  and  $^{238}\text{U}(n,f)/^{235}\text{U}(n,f)$ , indicating a systematic underestimation of the ratios. For neutron data standards, important reactions are fission reactions, where the PFNS shape is better known. Results corresponding to fission reactions have uncertainties lower or close to 1%.

## 2.6. Thermal neutron constants

Gilles Noguere and Ignacio Duran presented the status of the thermal neutron constants and integral references. Anton Wallner presented experimental results on  $^{235}\text{U}(n,f)$  related to  $^{238}\text{U}(n,\gamma)$  obtained in the meV energy range.

Various works performed over the last years (CONRAD analysis of the Axton's data, reference integral using EXFOR data, evaluation for ENDF/B-VIII.1 and JEFF4) allow to converge toward realistic "target values" for the capture, fission, elastic and total cross sections of  $^{233}\text{U}$ ,  $^{235}\text{U}$ ,  $^{239}\text{Pu}$  and  $^{241}\text{Pu}$ . These works confirm that the GMA analysis provide too high fission cross sections for  $^{235}\text{U}$  and  $^{239}\text{Pu}$ . However, the origin of this problem is not well understood.

Ignacio Duran recapitulated the procedure to define reference integrals for fissile actinide in the thermal and resonance ranges. This approach is interesting to get an estimate of the capture cross section because this reaction is difficult to estimate from experimental capture yield (due to self-shielding, multiple scattering, etc.). The method used in the thermal and resonance ranges was also applied to 2<sup>nd</sup> chance fission. The aim is to get an average cross section at 9 MeV and an integral value in the range [8-10 MeV]. Results for  $^{232}\text{Th}$ ,  $^{233}\text{U}$ ,  $^{235}\text{U}$ ,  $^{238}\text{U}$ ,  $^{237}\text{Np}$ ,  $^{239}\text{Pu}$ ,  $^{241}\text{Pu}$ ,  $^{241}\text{Am}$  and  $^{242m}\text{Am}$  were presented and discussed. The integral for the ratio  $^{238}\text{U}(n,f)/^{235}\text{U}(n,f)$  between 8 and 10 MeV is 2.015(8).

Anton Wallner started to present Maxwellian average cross sections (25 keV) performed at KIT using the activation technique (with  $^{197}\text{Au}$  for calibration) and offline AMS measurements (number of atoms). A similar technique was used to explore the meV energy range. Low neutron energy activation measurements were carried out at different reactors (FRM-II, ILL, BR-1). These experimental results will be useful for testing uranium evaluations. Note that for FRM-II, it is not a monoenergetic neutron beam. Therefore, the evaluation needs to be convoluted with the FRM-II neutron spectrum.

## 2.7. Codes and evaluation methods

Georg Schnabel, Denise Neudecker and Hiroki Iwamoto presented codes and methods of interest for improving the evaluation of the neutron standards.

Georg Schnabel gives a short history of the codes used within the Neutron Data Standard group:

- GMA: non-model Fortran code implementing the Generalized Least-Squares method, developed by W.P. Poenitz.
- GMAP: improved GLS algorithm to avoid PPP (Peelle's Pertinent Puzzle), implemented by S. Chiba, D. Smith and V. Proyaev.
- GMAPY: new python architecture for solving some data handling restrictions of GMAP.

GMAPY goes beyond the functionality of the GMA code by allowing for rigorous optimization of the likelihood function and the application of the Markov Chain Monte Carlo. The implementation of these capabilities was facilitated by using the TensorFlow and TensorFlow Probability Python packages. The new code can also read the GMA database stored as JSON file. For a more robust approach to code development, Git was adopted for version control of the GMAPY, and the code is also hosted on the GitHub platform. The development of GMAPY was done step by step to ensure that at each step the

code is functionally equivalent to the original GMAP code. However, local differences were observed between GMAP and GMAPY, such as for the resonance of  ${}^6\text{Li}$ . Asymmetric posterior distributions are also obtained (shift the central value compared to analytic model assuming Gaussian distributions).

The AIACHNE project aims to explore systematic biases in differential data by combining a machine learning technique with experimental data having minimal bias and past experiments. The present machine learning algorithm uses multiplicative basis functions to capture biases and relies on sparse Bayesian inference. Working on PFNS( ${}^{252}\text{Cf}$ ) shows that the algorithm was able to find the bias due to  ${}^6\text{Li}$  peak in Boldeman data (1986) around 0.2 MeV, using a medium-length bias function. The tool was trained on this problem in view of correcting data of this effect. In addition, statistical tests are available for example to indicate which type of bias dominate in a given population of data. This approach is promising for providing evaluation of many other PFNS.

Hiroki Iwamoto showed that Gaussian Process Regression (GPR) is a promising option for evaluations. Examples using different kernel functions to represent the correlation between training datapoints are presented. The obtained covariance matrices are rather different and led to different uncertainties. For example, in the case of GPR with Matern 3 kernel, stronger correlations are obtained at high energies compared to GLS, leading to smaller uncertainties.

## 2.8. Review of the GMA database

The in-person participants meeting was held between 10 a.m. and 2 p.m. It was devoted to the redetermination of the data status (mostly data type) of TOF measurement  ${}^{239}\text{Pu}(n,f)/{}^{235}\text{U}(n,f)$ . Many measurements were normalized to the thermal constant values and considered as absolute measurements. They should be considered as shape measurements. The results are summarized in an Excel table.

Ratio  ${}^{239}\text{Pu}(n,f)/{}^{235}\text{U}(n,f)$  around 1 MeV has an uncertainty lower than 1% (0.6%-0.8%). However, differences between absolute data around 1 MeV are quite large. Above 10 MeV, discrepancies between data increase and the central values around 14 MeV is becoming questionable. Normalization issues coming from  ${}^{239}\text{Pu}$ ,  ${}^{235}\text{U}$  or both were discussed. Various sources of uncertainties can exist such as chemistry of the sample (oxidation...), half life, detectors sensitive to anisotropy of the fission fragment emission. A comprehensive work on  ${}^{239}\text{Pu}$  was done by Denise Neudecker. Note that between 0.6 and 0.8 MeV, the STD values seem to be systematically lower than data.

Vladimir Pronyaev also presented a review of the latest measurements (light elements,  ${}^{238}\text{U}(n,f)$ ,  ${}^{238}\text{U}(n,\gamma)$ ,  ${}^{197}\text{Au}(n,\gamma)$ ,  ${}^{235}\text{U}(n,f)/{}^6\text{Li}(n,t)$ ,  ${}^{235}\text{U}(n,f)/{}^{10}\text{B}(n,\alpha)$ ,  ${}^{238}\text{U}(n,f)/{}^{235}\text{U}(n,f)$ ) performed at various facilities using time-of-flight technique ( $n_{\text{TOF}}$ , LANL with the NIFFTE-TPC, CSNS Back-n).

## 3. PRESENTATION SUMMARIES

Participants' presentation summaries are given below, including their most important statements and conclusions. Full versions of the individual presentations are available at:

<https://conferences.iaea.org/event/372/contributions/>

### 3.1. The hydrogen standards – The first and uniquely so, A.D. Carlson (NIST, USA)

Some of the first hydrogen total cross section measurements for neutrons were made for the Manhattan project by Bailey in 1943 at Los Alamos in the MeV energy region. Based on a paper by Barschall in 1940, Bailey knew the CMS angular distribution was nearly isotropic. Thus, with the total cross section for normalization, he obtained the hydrogen angular distribution as a “standard.” There was no dependence on any cross section in getting the hydrogen standard, it only depends on neutron counting ratios and measured quantities.

(Barschall, at Princeton, proved that the energy distribution of recoils in an ionization chamber or proportional counter is proportional to the differential cross section for scattering in the CMS. He made measurements with hydrogen in the MeV energy range and found the energy distribution was flat.)

Bailey made some of the first  $^{235}\text{U}(n,f)$  cross section measurements with a double ionization chamber with a well-defined hydrogenous foil on one side and a  $^{235}\text{U}$  deposit of known mass on the other side. Thus neutron fluence determination with the hydrogenous foil allowed the  $^{235}\text{U}(n,f)$  cross section to be determined. But it was relative to the hydrogen cross section.

Due to the simplicity of making ratio measurements to the  $^{235}\text{U}(n,f)$  cross section, a number of ratio measurements to the  $^{235}\text{U}(n,f)$  cross section were made during the Manhattan project. It was the first use of that cross section as a standard.

The method for measuring angular distributions by Barschall is limited in energy range. The problem is that the range of proton recoils is too large for high energy neutrons. Also edge effects and end effects are a problem. Use of scattering chambers leads to good measurements of hydrogen scattering angular distributions.

One of the first sources used for hydrogen data was the Gammel phenomenological model. It did well up to about 30 MeV for the total cross section. Angular distributions were not as well reproduced. The Hopkins-Breit (Yale) phase shift analysis was an improvement and was accepted for the hydrogen standard for ENDF/B-III through V. Phase shift analyses were also done by the Arndt group.

The most recent work on the hydrogen standard has been carried out at LANL using the EDA R-matrix program. The ENDF/B-VI through VIII hydrogen standards are from those analyses. An important problem now is getting hydrogen scattering values in the upper MeV energy region. For the ENDF/B evaluations, 20 MeV is the highest energy. Work is continued at LANL on the hydrogen evaluation by Paris and Hale. The analysis is now up to about 100 MeV with the objective of going up to 350 MeV. However, data above 20 MeV are not going to be officially available until the next standards evaluation is completed.

This raises the question what measurements should be used to determine the neutron standards in the high-energy range for the hydrogen standard in the high neutron energy region, above the 20 MeV limit that we have for the hydrogen standard. For the n\_TOF fission cross section work they have used the VL40 evaluation by Arndt for their data up to 450 MeV. However unfortunately there are differences for the various Arndt evaluations that were done 4 times a year, e.g. 6% at 120 MeV and at an angle of 150°. This leads to some loss of confidence in them.

It is suggested that experimental results be given in their primary form. For the fission data it would be absolute fission data divided by absolute proton rates. If comparisons to other data are required, clearly state what hydrogen evaluation was used to convert the ratio. Until the determination of accurate hydrogen data has been achieved, this is all you can do. When those data are available one can easily convert with a new hydrogen standard.

### 3.2. Progress on the development of gmapy, G. Schnabel (IAEA, Vienna)

The previous evaluations of the neutron data standards relied on the Fortran code GMAP [1] developed by Wolfgang Poenitz and further extended by V. Pronyaev and D. Smith [2]. This code reads all experimental data including uncertainties from the neutron data standards database and performs the Generalized Least Squares method (GLS) to obtain best estimates and associated covariance matrices. Recently, it was deemed beneficial to include ratios of spectrum averaged cross sections (SACS) [3] and the quantification of energy-dependent unrecognized sources of uncertainty [4] into the evaluation procedure. The Fortran code exhibits a convoluted code structure, making robust

developments challenging. Therefore, a new Python package [5] was conceived that can be run in a mode that is functionally equivalent to the Fortran code, which was proved by numerous test cases. In addition, it offers new possibilities for data access and analysis going beyond the Fortran version, which are:

- 1) Inclusion of ratio of SACS measurements into the evaluation;
- 2) Accounting and assessment of energy-dependent USU components;
- 3) Optimization-based as well as Monte Carlo based inference;
- 4) Users can easily retrieve data and covariance matrices for their own analysis.

**References:**

- [1] <https://nds.iaea.org/standards/Reports/extract-from-indc-usa-85.pdf>
- [2] <https://nds.iaea.org/standards/Reports/Min-Max-PPP.pdf>
- [3] [https://www.epj-conferences.org/articles/epjconf/abs/2023/07/epjconf\\_cw2023\\_00027/epjconf\\_cw2023\\_00027.html](https://www.epj-conferences.org/articles/epjconf/abs/2023/07/epjconf_cw2023_00027/epjconf_cw2023_00027.html)
- [4] <https://www.sciencedirect.com/science/article/pii/S0090375219300717>
- [5] <https://github.com/iaea-nds/gmapy>

**3.3. Progress on the validation of the Thermal Neutron Constants, G. Noguere (CEA, France)**

TABLE 1. Target values for the thermal neutron constants (TNC)

	<sup>233</sup> U	<sup>235</sup> U	<sup>239</sup> Pu	<sup>241</sup> Pu
$\sigma_{tot}$	≈590(2)	≈699.8(20)	≈1029(5)	≈1399(2)
$\sigma_f$	≈533(2)	≈586.2(30)	≈751(2)	≈1024(2)
$\sigma_\gamma$	≈45(1)	≈99.5(15)	≈270(3)	≈363(7)
$\sigma_n$	≈12.3(7)	≈14.1(2)	≈8(1)	≈11.9(25)
$\nu_{tot}$	2.484-2.490	2.414-2.436	2.868-2.878	2.940(13)
$I_3$		≈245.7(40)		

Questions about the experimental validation of the TNC arose as soon as the latest TNC were released in 2017. Indeed, issues were identified on the thermal fission cross sections of <sup>235</sup>U and <sup>239</sup>Pu. In order to solve the observed problems, the strategy consists in using feedback from independent works. For this purpose, we have considered the following results:

- CONRAD analysis of the TNC (Axton report and EXFOR data) using GLS and marginalization strategy [1];
- Reference integrals for fissile actinides from I. Duran using TOF data from EXFOR [2];
- Resonance parameters evaluated for the international libraries JEFF-4 (CONRAD analysis using EXFOR data) and ENDF/B-VIII.1 (SAMMY analysis using SAMMY database).

These different works allow establishing a set of “target values” for the capture, fission, elastic and total cross sections of <sup>233</sup>U, <sup>235</sup>U, <sup>239</sup>Pu and <sup>241</sup>Pu. For the total neutron multiplicity, rather than target values, it was mainly possible to guess a “confidence interval”. The compilation of these “target values” reported in Table 1 confirms that the GMA analysis provides too high fission cross sections for <sup>235</sup>U and <sup>239</sup>Pu. Unfortunately, the origin of this problem is not well understood. Therefore, the TNC evaluation should be considered as an independent work and not included in a fitting procedure that combines the full GMA database. An independent confirmation using e.g. GMAPy code will be useful.

**References:**

- [1] <https://www-nds.iaea.org/index-meeting-crp/TM%20STD%202016/docs/TM-STD-Noguere.pdf>
- [2] <https://www.sciencedirect.com/science/article/pii/S009037522400005X>

### 3.4. NIFFTE fissionTPC status update on $^{239}\text{Pu}(n,f)/^{235}\text{U}(n,f)$ and $^{235}\text{U}(n,f)/^6\text{Li}(n,f)$ cross section ratio measurements, M. Anastasiou, L. Snyder (LLNL, USA)

The presentation provided an update on ongoing efforts of the NIFFTE collaboration. The first part of the presentation dealt with the ongoing data analysis of  $^6\text{Li}(n,t)$  and was given by Maria Anastasiou. The second part was concerned with two measurements of the  $^{239}\text{Pu}(n,f)/^{235}\text{U}(n,f)$  ratio performed at LANL and was presented by Lucas Snyder.

Regarding the ongoing data analysis of  $^6\text{Li}(n,t)$  reaction up to 2-3 MeV using the TPC at LANL, efforts to improve the selection efficiency and to determine various corrections (wraparound, scattered neutrons, etc.) are in progress. One major selection efficiency correction appears at angles around 90 degrees where the loss of energy in the target is a significant effect. The preliminary data (after a wraparound correction) allow for the extraction of the angular distribution of emitted tritons, which shows good agreement with recent Bai data. It was also noted that one advantage of the fissionTPC experiment over experiments where detectors are placed at fixed angles is the large angular coverage and the possibility to obtain a nearly continuous distribution. The determination of additional corrections related to diffusion (due to fissionTPC angular tracking detector effects) and scattered neutrons is in progress. These corrections need to be carefully considered for each energy and angle-cosine bin. An appropriate detector response model in combination with data-driven simulations is helpful in this regard. Simulations showed that events related to wraparound can be well identified in a coordinate system with respect to alpha charge and track angle. The effect of diffusion and scattered neutrons will also be simulated.

The second part of the presentation elaborated on two measurements of the ratio  $^{239}\text{Pu}(n,f)/^{235}\text{U}(n,f)$  performed at LANL in the energy range from 100 keV to 100 MeV. After a brief review of the fissionTPC method itself, including essential publications, previous measurement results of the  $^{239}\text{Pu}(n,f)/^{235}\text{U}(n,f)$  ratio obtained within the NIFFTE collaboration were presented. These results are also documented in [1, 2] and deviate systematically from the ENDF/B-VIII.0 evaluation. They are therefore recommended to be used as shape data only. It was speculated that the systematic deviation may be due to a damaged target. Afterwards, the presentation elaborated in detail on the impact of the neutron flux profile and the overlap between beam and target (meaning the beam and the actinide target exhibit spatial non-uniformity). Based on these considerations, a data driven correction term named “U-corrected Pu-overlap Pu-overlap term” was derived. The form of this correction was well validated, which however does not rule out systematic offset due to “space-charge”. The possible magnitude of this offset was estimated to be around 0.5%.

The two new targets used for the measurement had a different size, which was seen as an opportunity to rigorously check assumptions in the data analysis. For the determination of the ratio, a different target size translates into a different normalization correction. The analysis of data collected with the silicon detector is ongoing. Compared to previous measurements, the tracking improved over the years and the distortions of the track angle are well understood. It was also noted that the track length resolution is much better than the energy resolution. The preliminary analysis indicated that the shape can be well determined, but absolute cross sections are still difficult to estimate as the uncertainty on the normalization factor is not well understood at this point. The next planned steps will therefore be a complete normalization analysis of the silicon detector data, the quantification of the space-charge effect (by further simulation and the collection of more radiograph data), and a radial cut variational analysis.

#### References:

- [1] L. Snyder, M. Anastasiou, N.S. Bowden, et al., Nucl. Data Sheets **178** (2021) 1-40
- [2] M. Monterial, K.T. Schmitt, C. Prokop, et al., Nucl. Instrum. Meth. A **1021** (2022) 165864.

### 3.5. New integral references for fissile actinides, I. Duran (USC, Spain)

#### 1. Introduction

The final accuracy of the evaluations relies on the quality of the experimental data being used. On the other hand, the quality of experimental datasets depends dramatically on its calibrations and normalizations with respect to the Standards. As a matter of fact, many experimental datasets in EXFOR are not well documented making the traceability with respect to any Standard not easy. A way to overcome this lack of information is by renormalizing the original dataset to well established references. Historically, the principal international Nuclear Data Standards are a few constants at thermal point that include the four main fissile actinides (see the TNC table in Ref. [1]). But for ToF experiments, there are often experimental problems in performing measurements with a neutron beam having exactly the thermal point energy of 25.3 meV. Therefore, in addition to reference values in the thermal energy range, it is also useful to have high accuracy integral values as reference at energies above a few 1eV that are more easily reachable in most of the ToF experiments. In a previous work [2] is described the procedure followed to adopt as Reference in the thermal energy range the integral values of the (n,f) cross-section for the four fissile major actinides ( $^{233}\text{U}$ ,  $^{235}\text{U}$ ,  $^{239}\text{Pu}$  and  $^{241}\text{Pu}$ ). The same procedure was also applied in the Resolved Resonance Range [3] for these major actinides, and, for convenience of use, the integral values of the reaction  $^{10}\text{B}(n,\alpha)$  are also included. This reaction meets all the requirements of an absolute Standard, being worth of more accurate measurements at different labs all around the world.

Concerning the (n,f) ToF measurements at higher neutron energy, the most important source of systematic error in the cross-section evaluations is the absolute normalization of every dataset, which was often performed by measuring simultaneously other isotopes as reference, using the integral value in a certain -not standard- energy interval of the corresponding datafile retrieved from an evaluated library. The choice of the energy interval used as integral reference has been left to the experimentalist's criteria, thus leading to a hardly assessable uncertainty. Using standard integration intervals, wide enough to get very low statistical uncertainties, should lead to a better normalization of every experimental dataset, thus reducing the associated total uncertainty of the evaluated datafiles. In this work the experimental datasets of the (n,f) cross section of actinides are reviewed looking for the best suited energy interval to be recommended for renormalization purposes. A common integration range from 8 to 10 MeV is proposed for the whole set of isotopes of highest interest for fission applications, falling between the second and the third chance thresholds where the (n,f) cross sections show a flat behavior.

#### 2. Integral cross-section References for the main Fissile Actinides (n,f) at low energies.

Here is a proposal for adopting as Reference values the integral data on (n,f) for the fissile major actinides ( $^{233}\text{U}$ ,  $^{235}\text{U}$ ,  $^{239}\text{Pu}$  and  $^{241}\text{Pu}$ ), as well as for the reaction  $^{10}\text{B}(n,\alpha)$  that is a Standard very often used as beam monitor in such a experiments. As these integral values depend on the Thermal Neutron Constants (TNC), also the ratios of these integrals to the thermal point values are given in this section.

The first step is to adopt the integration limits to get the references. The limits of the integrals *I* have been selected to be the same for every reaction, around the thermal point at 0.0253 eV. The integration limits for the RRR were adapted to each one actinide according to the shape of its (n,f) cross-section that show the different behavior of their resonances; they were chosen between two deep valleys having inside one or more high resonances, thus having a big integral value independent of energy miscalibrations. They are shown in the following table, as they were agreed in previous IAEA meetings (Ref. [4]):

Integration limits	<i>I1</i> : thermal range [meV]	<i>I3</i> : RRR [eV]
<sup>233</sup> U(n,f)	20 - 60	8.1 – 14.7
<sup>235</sup> U(n,f)	20 - 60	7.8 – 11
<sup>239</sup> Pu(n,f)	20 - 60	9.0 – 20.0
<sup>241</sup> Pu(n,f)	20 - 60	11.7 – 19.5

The evaluation of the integrals, *I1* and *I3*, has been done selecting those experimental datafiles retrieved from EXFOR having high resolution and covering the whole energy range from thermal to RRR, looking for ratios *I3/I1* that are independent of the normalization done by the experimentalists at the time of each experiment. The procedure used is described in Ref. [2].

In the next table are first the values of the ratios  $\sigma_0 / I1$  obtained by the procedure in Ref. [2]. The value of *I1* for each nuclide can be deduced immediately by using the corresponding cross-section value at the thermal point  $\sigma_0$  taken from the current TNC. In the second column are the values of the ratios *I3/I1* for the four main fissile actinides. The uncertainties quoted here come from the standard deviations of the different experiments with respect to their non-weighted mean value.

	$\sigma_0 / I1$ [1/eV]	<i>I3 / I1</i>
<sup>233</sup> U(n,f)	30.40(16) – 0.5%	39.31(54) – 1.4%
<sup>235</sup> U(n,f)	31.20(14) – 0.4%	13.08(20) – 1.5%
<sup>239</sup> Pu(n,f)	29.60(7) – 0.2%	41.65(22) – 0.5%
<sup>241</sup> Pu(n,f)	29.95(35) – 1.2%	40.46(85) – 2.1%

It is worth mentioning that those ratios including the values of  $\sigma_0$  refer to the current TNC table values, i.e., they must be scaled as the TNC values evolved. Then, the *I1* and *I3* values derived from the above listed ratios are fully traceable to the TNC table. They are given in the next Table:

	<i>I1</i> [b.eV]	<i>I3</i> [b.eV]
<sup>233</sup> U(n,f)	17.53(10) – 0.6%	689.0(10.8) – 1.6%
<sup>235</sup> U(n,f)	18.78(8) – 0.4%	245.7(4.1) – 4.1%
<sup>239</sup> Pu(n,f)	25.42(5) – 0.2%	1058.7(6.4) – 0.6%
<sup>241</sup> Pu(n,f)	34.05(47) – 1.4%	1377.8(33.1) – 2.4%

Finally, in the following table, the integral values of the reaction <sup>10</sup>B(n, $\alpha$ ) for the different energy intervals are included:

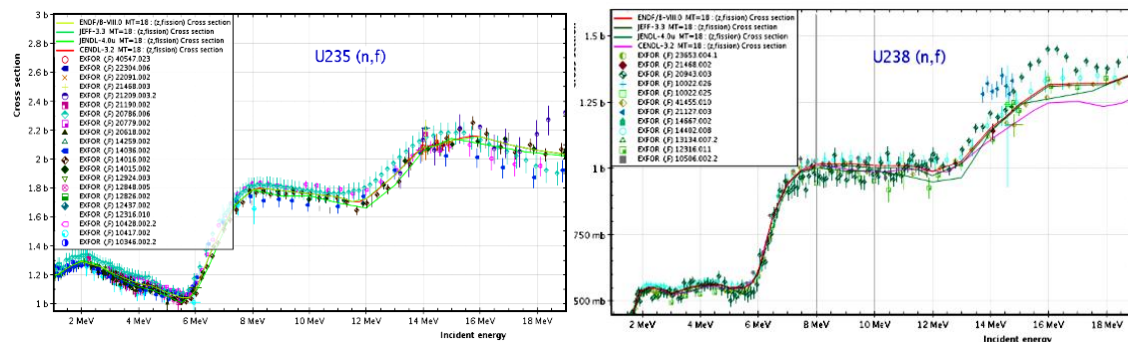
Integration limits	<i>I1</i> and <i>I3</i> for <sup>10</sup> B(n, $\alpha$ ) [b.eV]
20 – 60 meV	127(0.8%)
8.1 – 14.7 eV	640.67(0.9%)
7.8 – 11 eV	1208.5(0.9%)
9.0 – 20.0 eV	1800.7(0.9%)
11.7 – 19.5 eV	1217.5.(0.9%)

Note: The assigned uncertainties come from the USU of the <sup>10</sup>B(n, $\alpha$ )  $\sigma_0$  in the NDS2018 [1].

### 3. Integrals above threshold

Concerning the fission cross section of the actinides above threshold (around 1-2 MeV) the question now is to look for high quality integral references in order to improve the present standards and the evaluation of those actinides involved in the fast-reactors cycle. The first step is then to adopt the integration limits. For the whole set of the isotopes of most interest, defining a common integration range becomes useful because most of the experimental measurements have actually been done as cross-section ratios to  $^{235}\text{U}$  or  $^{238}\text{U}$ .

In the below figure the  $^{235}\text{U}(n,f)$  and  $^{238}\text{U}(n,f)$  cross-section profiles in the energy range from 1 to 19 MeV are shown, as retrieved from EXFOR, including both the main evaluated libraries and a selected set of high-resolution experimental datafiles (see EXFOR for references).

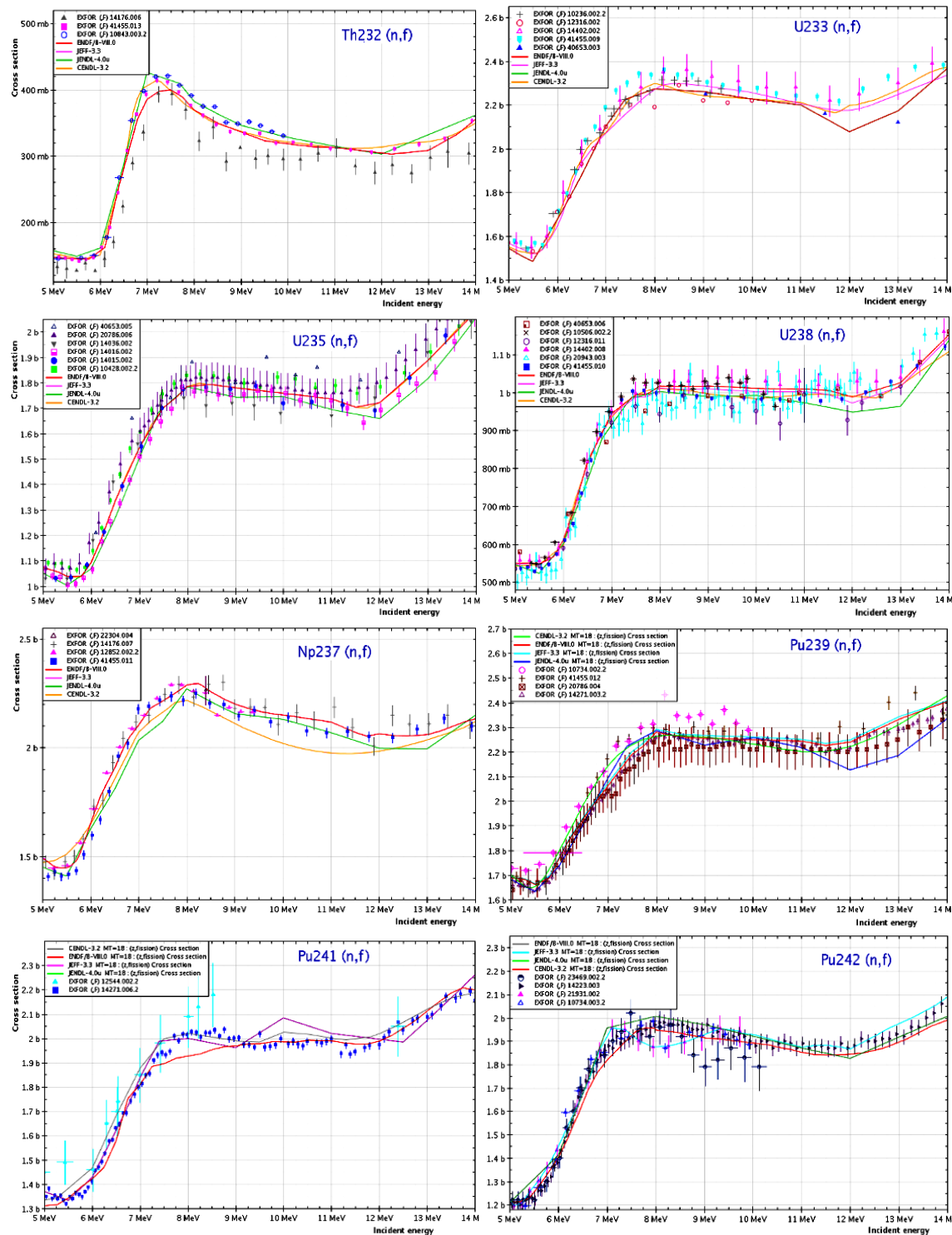


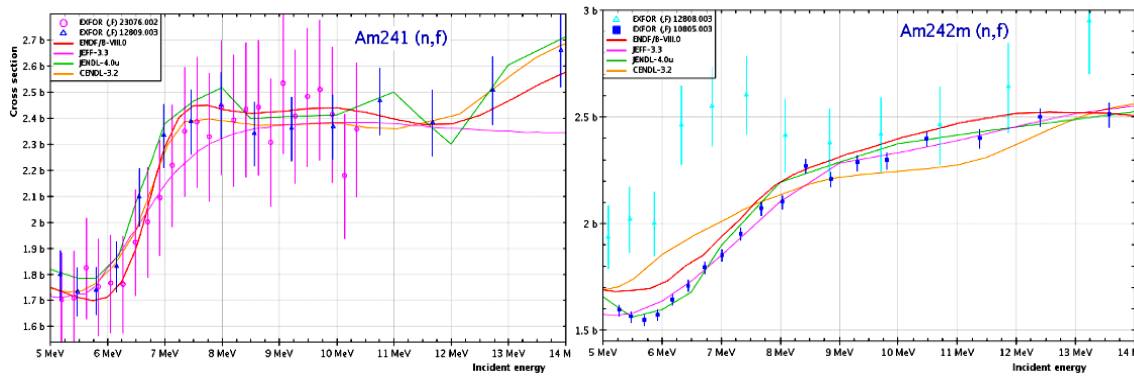
As it can be seen, for these two isotopes of Uranium there are two plateaus: one from 2 to 5 MeV and another going from 8 to 11 MeV. Both are well suited to be adopted as integral references. In principle, the first one is better because there are several good experiments using the neutron spectrum of Cf sources which is well centered inside it [5]. On the other hand, the second interval, in-between the second and the third chance thresholds, is flatter and is showing higher values of the (n,f) cross section. Such a profile can be easily fitted to a straight-line segment with a low slope, thus giving an integral value little sensitive to energy miscalibrations. If one takes into consideration the need of extending the interval selection to other actinides, the second interval is better because the first plateau is not so well defined for most of them, showing lower values of the fission cross section. Moreover, the sharp changes of the fission-fragments anisotropy observed in this energy region is a challenge for the experimental detection setups. In consequence, it is proposed to adopt as integral reference the energy interval from 8 to 10 MeV, where the approximation to a straight-line behavior can be sustained for the whole set of the actinide isotopes most involved in the fast neutron fission reactors.

Therefore, in this work, the evaluation of the integrals for the most relevant nuclides involved in the fast neutron fission reactors is done selecting only those experimental datafiles retrieved from EXFOR that cover the afore mentioned energy-range with a high resolution (namely,  $^{232}\text{Th}$ ,  $^{233-235-238}\text{U}$ ,  $^{237}\text{Np}$ ,  $^{239-241-242}\text{Pu}$ , and  $^{241-242\text{m}}\text{Am}$ ). They were measured by the neutron time-of-flight (ToF) method at experimental facilities having a white spectrum neutron flux monitored using a well-known reference target, that in most cases was  $^{235}\text{U}$ . Their cross-section profiles are shown in the next figure (see EXFOR for references). It is worth mentioning that most of the  $^{235}\text{U}(n,f)$  experimental datasets were in turn normalized with reference to the  $^1\text{H}(n,e)$  reaction, whose evaluation has evolved in time. Consequently, the accuracy of these measurements is constrained by both the accuracy of the reference dataset, and the accuracy of the neutron energy calibration (ToF). These two constraints are, in this work, the most relevant components of the systematic uncertainties. In comparison to these two systematic components, the uncertainty component reflecting the statistical errors can be neglected due to the large number of data points inside the integration interval.

Concerning the first constraint, the normalization of the cross-section values was done by the authors of the experimental works, as retrieved from EXFOR, involving a factor that has changed with time as the nuclear data standards have been updated (see [1] and [6]). The second constraint is not relevant

in this evaluation procedure as long as, in the selected integration interval (from 8 to 10 MeV), the cross section behavior is more or less flat, and so little sensitive to energy miscalibrations. Moreover, the statistical spread of the cross-section values inside the integration interval is dramatically reduced after being fitted to a straight line.





Conversely to those evaluations based on the point-wise approach, this evaluating procedure is based on the fittings to straight-lines of the experimental data inside the chosen integration interval. So that only those datafiles in EXFOR containing enough points inside this energy interval can be selected. Therefore, every retained datafile gives us directly the cross-section value at 9 MeV and the integral value in the 8 -10 MeV interval. Then, each value so obtained has been renormalized by a factor that comes from the updating of the monitoring value taken by the authors, as declared in the corresponding EXFOR records.

As above mentioned, most of the EXFOR datasets comes from experiments using as reference the  $^{235}\text{U}(n,f)$  reaction, which is IAEA Standard. Therefore, the final accuracy of the integral values relies on the goodness of the straight-line approach, as well as on the integral value being adopted for  $^{235}\text{U}$ , having one uncertainty that according to the Nuclear Data Standards (NDS2017) [1] is dominated by the unknown systematic components (USU) coming from the historical  $^{235}\text{U}(n,f)$  measurements. It is worth noting that the  $^{238}\text{U}(n,f)$  reaction has also been adopted as IAEA Standard because, as a matter of fact, the best measured quantity is the ratio of both cross sections that was discussed in the paper on USU [7] where different statistical models were used to analyze a selected set of experimental cross sections retrieved from EXFOR. The conclusion was that a value of this ratio of 0.572 can be adopted with an uncertainty of 0.3%. In this work we found now that the mean value of the ratios at 9 MeV obtained by fitting the 12 datasets retrieved from EXFOR give us a value of 0.570, with 1.1% of statistical standard deviation. This value also agrees well with the ratio of 0.571 obtained from the fitting of the GMA nodes in the IAEA Standards [1], which is proof in favor of the reliability of the fitting to straight-lines procedure.

On the one hand, from using the five  $^{235}\text{U}(n,f)$  cross section experimental datasets retained from EXFOR after renormalization, the mean value at 9 MeV is 1.763(19) b, whereas the corresponding mean value found from the main evaluated libraries is 1.769(9) b. One can see that the difference is minimal and well inside the standard confidence intervals. Therefore, the value that has been adopted to obtain the cross section for each nuclide from their ratio to  $^{235}\text{U}$  is a conservative 1.766(10) b for the whole set of actinides. Obviously, if a different  $^{235}\text{U}$  value is used as reference the so obtained values should be changed accordingly. For instance, for  $^{238}\text{U}(n,f)$ , if its ratio to  $^{235}\text{U}(n,f)$  is 0.572, its cross section value at 9 MeV should be 1.010 b, in good agreement with the NDS point-wise value of 1.017(14) b, and also with the mean value given by the main evaluated libraries of 1.003(10) b.

It is worth noting that the main goal of this work is not to improve the evaluations of the different fission cross sections here included. No matter what the  $^{235}\text{U}$  integral reference value is, what is important is to introduce the procedure giving integral reference values above 1 MeV.

The next Table lists the values of the cross section at 9 MeV obtained for the whole set of actinides by integration in the 8 to 10 MeV energy interval. All these values have been calculated by taking the non-weighted mean of the straight-line fits (both for the datasets in EXFOR and for the evaluated libraries).

	XS [b] at 9 MeV			
	From EXFOR (XS renorm.)	From EXFOR (Ratios to U5)	Evaluated libraries Point value	Fitted value
<sup>232</sup> Th	0.339(9)	0.344(8)	0.339(5)	0.342(6)
<sup>233</sup> U	2.289(38)	2.286(54)	2.262(19)	2.259(11)
<sup>235</sup> U	1.763(19)	-----	1.771(19)	1.769(9)
<sup>238</sup> U	1.003(18)	1.007(12)	1.004(12)	1.003(9)
<sup>237</sup> Np	2.239(47)	2.200(63)	2.168(46)	2.185(50)
<sup>239</sup> Pu	2.263(46)	2.239(52)	2.253(16)	2.262(8)
<sup>241</sup> Pu	2.01(###) <sup>1</sup>	1.992(15)	1.970(13)	1.994(22)
<sup>242</sup> Pu	1.908(32)	1.896(34)	1.950(22)	1.943(32)
<sup>241</sup> Am	2.417(3)	2.568(264)	2.396(27)	2.397(34)
<sup>242m</sup> Am	2.329(80)	2.321(84)	2.273(38)	2.257(45)

The next Table lists the integral values of the cross sections in the energy interval from 8 to 10 MeV obtained from the mean values of the straight-line fits applied to: the experimental datasets, the measured ratios to <sup>235</sup>U (taking 1.766 b as the <sup>235</sup>U (n,f) value at 9 MeV), and to the datasets retrieved from the major evaluated libraries, after applying the same fitting procedure.

	Integral 8-10 MeV [b·eV]		
	From EXFOR (XS renorm.)	From EXFOR (Ratios to U5)	Evaluated libraries
<sup>232</sup> Th	0.679(17)	0.688(16)	0.684(12)
<sup>233</sup> U	4.578(76)	4.572(108)	4.519(22)
<sup>235</sup> U	3.527(38)	-----	3.537(18)
<sup>238</sup> U	2.006(35)	2.011(24)	2.007(18)
<sup>237</sup> Np	4.478(93)	4.399(125)	4.370(99)
<sup>239</sup> Pu	4.526(91)	4.478(104)	4.523(15)
<sup>241</sup> Pu	4.03(###) <sup>1</sup>	3.984(30)	3.988(44)
<sup>242</sup> Pu	3.815(64)	3.792(67)	3.886(63)
<sup>241</sup> Am	4.834(3)	5.135(529)	4.794(67)
<sup>242m</sup> Am	4.658(160)	4.643(167)	4.514(89)

The quoted uncertainties come from the statistical standard deviations of the different experiments with respect to their non-weighted mean value. The values in this Table are generally in good agreement with each other. Nevertheless, there are notable discrepancies between the different evaluated libraries, as can be seen also in the above shown cross-section graphs. This is pointing to the need to redo the evaluations including a denser grid of points from 5 to 12 MeV.

#### 4. Conclusions

This work presents a procedure to obtain the integral cross sections from the straight-line fits in the energy range from 8 to 10 MeV for a wide set of actinide isotopes of relevance for the study of fast

<sup>1</sup> The estimate for <sup>241</sup>Pu taken from EXFOR is based on a single point, hence the standard deviation cannot be determined, which is indicated by “###”.

fission reactors (namely,  $^{232}\text{Th}$ ,  $^{233,235,238}\text{U}$ ,  $^{237}\text{Np}$ ,  $^{239,241,242}\text{Pu}$ , and  $^{241,242\text{m}}\text{Am}$ ). The proposed integrating interval is the same for the whole set of isotopes, falling in-between the second and the third chance thresholds, where the approximation of a straight-line behavior can be sustained. The results prove that, in this energy range, the error introduced by this approximation is lower than the uncertainties found in the evaluations based on point-wise methods.

The integral references that have been found for each nuclide should help to better renormalize the corresponding evaluated datafiles, even though (despite?) the strong correlation with the integral value found for  $^{235}\text{U}$ . From the values here obtained, a value of its cross section at 9 MeV of 1.766 b is proposed as reference, giving an integral cross section of 3.532 b-eV in the 8 to 10 MeV interval, according to the straight-line fit procedure.

### References

- [1] A.D. Carlson, V.G. Pronyaev, R. Capote et al., Evaluation of neutron data standards, Nucl. Data Sheets **148** (2018) 142–187.
- [2] I. Duran, R. Capote, and P. Cabanelas, Normalization of ToF (n,f) Measurements in Fissile Targets: Microscopic cross-section integrals, Nucl. Data Sheets **193** (2024) 95-104.
- [3] Neutron Data Standards, Summary Report of the IAEA Technical Meeting, 18-21 Oct 2022, D. Neudecker, G. Schnabel (Eds), Report INDC(NDS)-0865, Vienna, Austria, October 2023
- [4] The International Nuclear Data Evaluation Network (INDEN) on Actinide Evaluation in the Resonance Region (3), Summary Report of the IAEA Consultants Meeting, 17-19 Nov 2020, G. Noguere, R. Capote (Eds), INDC(NDS)-0818, Vienna, Austria, July 2021,
- [5] R. Capote, G. Schnabel, A.D. Carlson, V.G. Pronyaev, G. Noguere, and D. Neudecker, Experimental spectrum averaged cross sections (SACS) in  $^{252}\text{Cf(sf)}$  neutron field and its impact on the evaluation of neutron standards, EPJ Web of Conferences **281** (2023) 00027.
- [6] A.D. Carlson, V.G. Pronyaev, D.L. Smith, et al., International evaluation of neutron cross section standards, Nucl. Data Sheets **110** (2009) 3215–3324.
- [7] R. Capote, S. Badikov, et al., Unrecognized Sources of Uncertainties (USU) in Experimental Nuclear Data, Nucl. Data Sheets **163** (2020) 3215–3324.

### 3.6. Ratios of the cross sections for the $^{10}\text{B}(n,\alpha)^7\text{Li}$ reaction to the $^6\text{Li}(n,t)^4\text{He}$ reaction, J. Liu (Peking University, China)

As we all know, neutron cross-section standards are the basis for measurements and evaluations of nuclear data. In 2019, we measured the differential and angle-integrated cross sections of the  $^6\text{Li}(n,t)^4\text{He}$  and  $^{10}\text{B}(n,\alpha)^7\text{Li}$  reactions in the 1.0 eV – several MeV region based on the CSNS Back-n white neutron source [1, 2]. However, in our published measurement data, the relative neutron flux of CSNS Back-n was measured using the  $^{235}\text{U}(n, f)$  reaction, which introduced relatively big uncertainties due to the resonance peaks in the  $^{235}\text{U}(n, f)$  cross sections, especially in the 1.0 eV – 1.0 keV neutron energy region. The experimental conditions for the measurements of the two reactions were the same. Therefore, we reanalyzed the experimental data and obtained the ratios of the cross sections for the  $^{10}\text{B}(n,\alpha)^7\text{Li}$  reaction to the  $^6\text{Li}(n,t)^4\text{He}$  reaction to avoid the big uncertainties from neutron flux.

As shown in Fig. 1a, the uncertainties of the present ratios are much smaller than those of other existing measurements. Furthermore, the present results cover a large neutron energy region from 1.0 eV to several MeV and they are in good agreement with the evaluation data of ENDF/B-VIII.0 and JEFF-3.3 libraries. Compared with our previous work, in the neutron energy region from 1.0 eV to 1.0 keV, the relative uncertainties of the present ratios are significantly smaller than those of our previous measurement data. In the 1.0 keV – 0.5 MeV region, the relative uncertainties of the present ratios come close to those of our previous measurements data, as shown in Fig. 1b. The ratios of the angular differential cross sections for the  $^{10}\text{B}(n,\alpha)^7\text{Li}$  reaction to the  $^6\text{Li}(n,t)^4\text{He}$  reaction were also obtained, which are in good agreement with the evaluations.

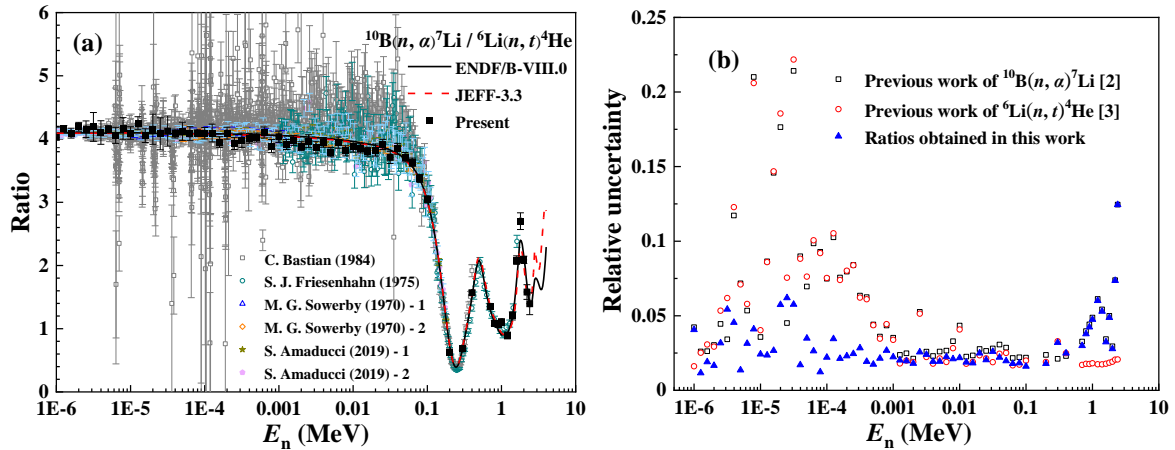


FIG 1. The ratios of the cross sections for the  $^{10}\text{B}(n,\alpha)^7\text{Li}$  reaction to the  $^6\text{Li}(n,t)^4\text{He}$  reaction (a) and their relative uncertainties (b).

## References

- [1] H. Jiang, et al., Chinese Phys. C **43** (2019) 124002 (in plot (b): [2]).  
 [2] H. Bai, et al., Chinese Phys. C **44** (2020) 014003 (in plot (b): [3]).

### 3.7. Measurement of the fission cross-section of $^{235}\text{U}$ relative to n-p scattering from 10 to 70 MeV at CSNS Back-n, Y. Chen (IHEP/CAS, China)

In this presentation, the measurement of the  $^{235}\text{U}(n,f)$  cross-section relative to n-p elastic scattering from 10 to 70 MeV was presented. This measurement was performed at the China Spallation Neutron Source (CSNS) back-streaming neutron line (Back-n). First, we gave a brief introduction for the CSNS and Back-n facility, including the CSNS-II upgrading project. Then the experimental setup was shown, which mainly consisted of a fission chamber (named FIXM) and a proton recoil telescope (PRT). The fission of  $^{235}\text{U}$  was measured by the FIXM. A PRT, composed by a silicon (300  $\mu\text{m}$  thick) and a CsI scintillator (3 cm thick), was used for extracting the neutron flux by measuring the n-p scattering. Two approaches were used when we were dealing with the n-p scattering cross-section. The first method was that the (angle integrated) H(n,n) cross-section was used and the effective efficiency (taking into account the angular distribution and geometric structure) was simulated by Geant4. The second method was directly using the differential H(n,n) cross-section given by Anrdt's solution. The preliminary results of  $^{235}\text{U}(n,f)$  cross-section from 10 to 70 MeV was obtained. Since the exact sample quantity inside the beam map is uncertain, the results were normalized to the IAEA standard integral value in 10-12 MeV. More detailed analysis will be done to improve the data quality.

### 3.8. Absolute cross section of the $^{235}\text{U}(n,f)$ in the energy range between 20 and 450 MeV at CERN n\_TOF, A. Manna (UNIBO, Italy)

The  $^{235}\text{U}(n,f)$  cross section is a fundamental benchmark for nuclear physics. It is widely used as main reference for nuclear reaction studies. This cross section is standard at thermal neutron energy and in the interval between 0.15 and 200 MeV, together with its integral value between 7.8 and 11 eV. Despite this widespread interest, in the energy range from 20 to 200 MeV only one experimental measurement from Lisowski (1991) and a few isolated points for quasi-monoenergetic neutron beam from Nolte (2007) are reported in the literature. Thanks to the availability of high energy neutrons together with the good energy resolution and the high instantaneous flux, the n\_TOF facility offers the possibility to fill this lack of experimental data. Therefore, an accurate and precise measurement was carried out with the aim of providing new data from 10 MeV to about 500 MeV.

To ensure the reliability of the cross section data obtained for these high neutron energies, a redundant experimental setup was employed. This allowed for cross-checking results from

independent systems in the low-energy region (up to 150 MeV). The setup consisted of three flux detectors and two fission detectors, enabling simultaneous measurement of both fission events and neutron flux incident on  $^{235}\text{U}$  samples as a function of neutron energy.

More specifically, to determine the number of fission events, the fission fragments (FFs) originating from the nuclear reactions in  $^{235}\text{U}$  were detected by a Parallel Plate Ionization Chamber (PPIC) operated based on the detection of a single fragment, whereas a Parallel Plate Avalanche Counters (PPACs) recorded both fragments simultaneously.

The two distinct detection strategies, PPAC and PPIC, result in different performance characteristics. PPAC, with its lower efficiency of around 60%, is well-suited for detecting neutrons up to 1 GeV. PPIC, on the other hand, offers near-perfect efficiency but is limited to neutrons below 150 MeV due to its higher gas pressure and specific construction.

For the determination of the absolute neutron flux, two types of detectors were developed, both based in the  $\Delta E$ -E matrix analysis: a Triple Stage Recoil Proton Telescope (3S-RPT) and two Multiple-Stage Recoil Proton Telescopes (MS-RPTs). The detection technique exploits the well-established neutron-proton elastic scattering cross section. A polyethylene sample is positioned in the beam, and three telescopes are placed at a fixed angle to detect protons emitted from the sample. The coincidence technique is employed to discriminate against background events not originating from the sample.

Due to the presence of carbon in the sample, dedicated background measurements and extensive Monte Carlo simulations were conducted to assess the impact of n-C reactions on the flux measurement. The key distinction between the two detectors is the method used to subtract the carbon contribution, which ultimately limits the maximum detectable proton energy to approximately 450 MeV for MS-RPT and 150 MeV for 3S-RPT.

Two completely independent set of results were obtained: one in which the cross section was extracted with the PPIC and the 3S-RPT, and one using the PPAC in combination with the MS-RPT. The two sets of cross section data, without any normalisation, proved to be in agreement, within the systematic uncertainties, over the entire energy-spectrum in which the two results overlap, i.e. from 40 MeV up to 150 MeV.

The evaluation of the systematic uncertainties was performed considering several contributions. Firstly, for the detection of the fission events, the sample mass, the effective density and the detection efficiency were assessed taking into account their corresponding uncertainty. Then, the uncertainty budget of the flux measurement was divided into correlated and uncorrelated factors. The first category includes the uncertainty related to polyethylene (and carbon) samples determined by the chemical composition, assessed after precise analysis of the samples. Then, the positioning of the samples in the beam which influences the geometric efficiency and differential n-p cross-sectional area have been considered. In the category of uncorrelated uncertainties there are the geometrical efficiency of the recoil proton telescopes as well as all the corrections applied in the analysis, i.e. event selection and dead-time correction.

The obtained cross section was compared with the evaluations and the data present in the literature, showing a good agreement with both. The cross section was additionally compared with theoretical calculations obtained with INCLXX/Abla07, defining the necessary modifications to the values of the parameters such as the height of the fission barrier and the level density of fission remnants, capable of reproducing the experimental result in the energy region between 150 and 450 MeV.

### 3.9. Angular distribution measurements of neutron elastic scattering by natural carbon at GELINA with the ELISA setup, G. Noguere (CEA, France)

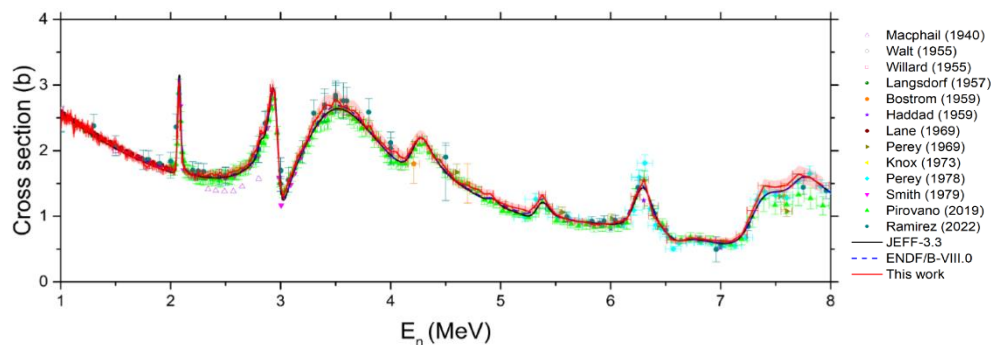


FIG 1. Elastic scattering cross section of natural carbon measured at JRC-Geel (red line) compared to EXFOR data and evaluations.

The scattering angular distributions (SAD) of natural carbon were measured at the GELINA facility of JRC-Geel with the ELISA detector [1]. The detection set-up is composed of 32 detectors located at 27 m from the neutron source. Measurements were performed relatively to  $^{235}\text{U}(n,f)$ . This set-up allows obtaining SAD for 8 angles (16.2°, 37.2°, 58.3°, 79.4°, 100.6°, 121.7°, 142.8°, 163.8°) from 1 to 8 MeV. The reconstructed angle-integrated cross section (Fig. 1) is in excellent agreement with the ENDF/B-VIII.0 evaluation. These new data will help to slightly improve the evaluated cross sections at backward angles. The data will be available via EXFOR in 2025.

#### References:

- [1] <https://journals.aps.org/prc/abstract/10.1103/PhysRevC.110.034609>

### 3.10. A comparison of Gaussian process regression with GLS results for $^{235}\text{U}(n,f)$ cross section, H. Iwamoto (JAEA, Japan)

The results of neutron-induced fission cross sections of  $^{235}\text{U}$  ( $150 \text{ keV} < E < 200 \text{ MeV}$ ) estimated by the Generalized Least Squares (GLS) method and the Gaussian Process Regression (GPR) method were compared. The comparison showed that the cross sections and their covariances estimated by the two methods generally agree at the evaluation energy points. GPR may be useful for validating the gmapy code, which uses GLS for the cross section evaluation, and for cross-checking the evaluated cross sections.

### 3.11. Impact and utility of SACS, R. Capote (IAEA)

The  $^{252}\text{Cf}(s,f)$  prompt fission neutron spectrum (PFNS) is a well-established standard neutron field with relatively low uncertainties evaluated by Mannhart in 1989 based on time-of-flight measurements. Therefore, measurements of spectrum-average cross sections (SACS) of  $^{235}\text{U}$ ,  $^{238}\text{U}$ ,  $^{239}\text{Pu}$  neutron-induced fission cross sections and their ratios in the  $^{252}\text{Cf}(s,f)$  neutron spectrum are very valuable information for the determination of the normalization factors of neutron induced fission cross sections of  $^{235}\text{U}$ ,  $^{238}\text{U}$  and  $^{239}\text{Pu}$  shape measurements and shape ratio measurements. Evaluated SACS values based on an updated version of the experimental database used by Mannhart (IRDF-2002) were presented, considering 13 datasets with SACS measurements of  $^{235}\text{U}(n,f)$ ,  $^{238}\text{U}(n,f)$ ,  $^{239}\text{Pu}(n,f)/^{235}\text{U}(n,f)$  and  $^{238}\text{U}(n,f)/^{235}\text{U}(n,f)$ . For this exercise, original Mannhart's evaluation code was used. Notably, both the evaluation of Mannhart performed in 2008 and the presented evaluation with updated experimental uncertainty assumptions are consistent with each other for the SACS ratio  $^{239}\text{Pu}(n,f)/^{235}\text{U}(n,f)$  values, being 1.504 and 1.495, respectively. In contrast to that, this SACS ratio was determined to be about 1.464 in the standards 2017 evaluation---significantly underestimating Mannhart's evaluation if considering evaluated uncertainties. Resolving this inconsistency is an

important concern in the neutron standards project. One step towards this goal is the inclusion of SACS ratio measurements in the standards database. Thanks to the new capabilities of the GMAPY code (a modernized version of the GMA code written in Python), this inclusion is possible now. Preliminary results using the improved datasets indicate an increase of the  $^{239}\text{Pu}(n,f)$  cross section, improving the consistency with Mannhart's evaluation. Further work is necessary, but the presented results indicated that the inclusion of revised SACS experimental values and ratio of SACS values will help improving the standards evaluation. Apart from SACS measurements in the  $^{252}\text{Cf}(s.f.)$  neutron spectrum, there are also SACS measurements in the  $^{235}\text{U}(n_{th},f)$  neutron field available, whose inclusion needs also to be considered. The expected impact on the evaluated  $^{239}\text{Pu}(n,f)$  fission cross section in the first-chance fission plateau is about 1% higher than the 2017 evaluated cross section. The impact of the PFNS uncertainty on the evaluated SACS is almost negligible.

### 3.12. Spectrum related SACS uncertainties, D. Smith

A calculated neutron spectrum-average cross section (SACS) is obtained by integrating the product response function of an evaluated differential cross section and the normalized neutron spectrum representation over a neutron energy range that encompasses non-negligible values of this product function. The uncertainty in a calculated SACS can be derived by applying the well-known "sandwich rule" to discrete representations of the cross section and spectrum covariance matrices. The cross-section uncertainty covariance matrix is weighted by the spectrum values while the spectrum covariance matrix is weighted by the cross-section values. The total SACS uncertainty is the sum of two independent terms, since the  $^{252}\text{Cf}(s.f.)$  neutron spectrum is considered in the present investigation and its covariance matrix is independent of that for all the reaction cross sections due to the way in which this well-studied spectrum has been evaluated.

SACS values and their uncertainty components have been calculated for a large number of neutron-induced reactions by Andrej Trkov using evaluated values produced for the neutron dosimetry library IRDFF-II [1, 2]. Evaluated information in this library is consistent with both ENDF/B-VIII.0 and the International Standards Library for reactions and energies where there is overlap of the respective contents. These SACS data were made available to the present author by Roberto Capote [3].

The present work involved assembling, organizing, and plotting this information according reaction type and a parameter referred to as E-50%. For any specific neutron reaction, this parameter corresponds to that neutron energy such that 50% of the normalized spectrum response comes from energies below this energy and 50% comes from above this energy. The results from this investigation are documented in detail in an IAEA report by the present author [4].

It is shown that the spectrum-related SACS uncertainty values for the IRDFF-II evaluated cross sections increase smoothly as a function of E-50% (with only a few exceptions) from near zero for E-50% around 2 MeV up to 30% for E-50% = 18 MeV, irrespective of details in the shapes of cross sections with similar E-50% values. However, the spectrum-related SACS uncertainties for reactions with E-50% below 2 MeV scatter considerably, although they are all below 1% in this region. The very small spectrum-related uncertainties for E-50% near 2 MeV in calculated SACS are due, in part, to uncertainty cancellation effects related to the normalized  $^{252}\text{Cf}(s.f.)$  spectrum.

#### References:

- [1] International Reactor Dosimetry and Fusion File, IRDFF-II, January 2020, Nuclear Data Services, International Atomic Energy Agency, <https://www-nds.iaea.org/IRDFF/>.
- [2] Andrej Trkov, et al., IRDFF-II: A New Neutron Metrology Library, Nucl. Data Sheets **163** (2020) 1-108.
- [3] Roberto Capote, IAEA Nuclear Data Section, private communication (2022).

- [4] Donald L. Smith, Observations on the Effects of  $^{252}\text{Cf}$  Spontaneous-Fission Neutron Spectrum Uncertainties on Uncertainties in Calculated Spectrum-Average Cross Sections for Reactions in the Neutron Dosimetry Library IRDFF-II, Report NDC(NDS)-0864, IAEA Nuclear Data Section, Vienna, Austria, 2022, <https://www-nds.iaea.org/publications/indc/indc-nds-0864/>.

### 3.13. $^{235}\text{U}$ and $^{238}\text{U}$ capture at thermal and sub thermal neutron energies, A. Wallner (HZDR, Germany)

Accelerator mass spectrometry (AMS) is used to quantify the long-lived reaction products  $^{236}\text{U}$  and  $^{239}\text{Pu}$ , both long-lived radionuclides that are products in the neutron capture reactions on  $^{235}\text{U}$  and  $^{238}\text{U}$  (via decay of short-lived  $^{239}\text{U}$  and  $^{239}\text{Np}$ ), respectively. The latest work and status of this new neutron capture cross section measurement for  $^{235}\text{U}(n,\gamma)$  at ultra-cold, cold and thermal neutron energies using AMS was presented. The method applied is a combination of neutron activation at different reactors and subsequent AMS measurements of the reaction product. Overall, activations were conducted at Mol/Belgium for thermal energy, at MLL (Munich, Germany) and ILL (Grenoble, France) with cold neutrons (two different mean energies each), and one irradiation at ILL with ultra-cold neutrons. Accordingly, these activations cover six energy points with an energy range from 50  $\mu\text{eV}$  to thermal. All irradiations and AMS measurements are finished now. The main outcome is, that the cross section data show a significant deviation of  $1/v$  for the  $^{235}\text{U}$  capture reaction. These data were normalized to  $^{238}\text{U}(n,\gamma)$  which is believed to exhibit a pure  $1/v$  dependence. Using  $^{\text{nat}}\text{U}$  samples allowed to study the  $^{238}\text{U}(n,\gamma)$  reaction in parallel in the same samples for all activations. Minor work is necessary for small adjustments when taking into account the finite neutron energy distributions for some irradiations – to allow for a direct comparison with the existing libraries. In general, deviations of the new experimental data for  $^{235}\text{U}(n,\gamma)$  to the existing data in the libraries are clearly seen. A publication is now drafted.

### 3.14. AIACHNE work towards a new $^{252}\text{Cf}(sf)$ PFNS evaluation, D. Neudecker (LANL, USA)

This talk focuses on work towards a new  $^{252}\text{Cf}$  PFNS evaluation. To this end, we reviewed 26 datasets (50 total if one counts all sub-sets). Mannhart accepted only data by Blinov (1973), Boettger (1983), Boldeman (1986) (low and high  $E_{\text{out}}$ ), Dyachenko (1989) (called Lajtai by Mannhart), Maerten (1984) and Poenitz (1982). He has mentioned in a presentation at a standard meeting that he would recommend adopting data by Chalupka (1990) and Maerten (1990). The data by Blain (2017), Bowman (1985), Gook (2014), Kornliov (2015) and Lajtai (1990) were also published after the evaluation of Mannhart. Out of the datasets accepted by Mannhart, we would replace the data by Dyachenko (1989) with those from Lajtai (1990). They are from the same group and based on the same raw data but data by Lajtai (1990) represent the final dataset (correcting for issues in detector response affecting Dyachenko (1989) data). Currently, we would reject Boldeman (1986)  $^6\text{Li}$  data because of the strong bias around the  $^6\text{Li}$  resonance in the data that could bias the evaluation. Maerten (1984) data will be replaced by Maerten (1990). The reason for that is the use of a circular argument for obtaining the detector response: An evaluated  $^{252}\text{Cf}$  PFNS was used to derive the detector efficiency for 1984 data biasing the experimental data to that evaluation. This shortcoming does not apply to the well-measured data of Maerten (1990).

We also accept data by Boytsov (1983) and Blinov (1980) that were not accepted by Mannhart. Blinov did not state explicitly for that dataset if angular distribution correction had been undertaken which could have possibly led to their rejection. However, that correction was undertaken for the 1973 data, and we assume the same applied for 1980 data. We are not sure what led to the rejection of Boytsov data but deem them well-measured and analysed. Blinov data will allow the evaluation to extend to lower energies while Boytsov data will reduce uncertainties from 100 keV to 4 MeV. In addition to that, we accept Chalupka (1990) data. Kornilov (2015) data were only accepted as validation

measurement at the time of the standard meeting. There was considerable discussion on the dataset and after the meeting the AIACHNE team followed up with Prof. Tom Massey on the data and could resolve some questions and uncertainty issues with the data. So, part of Kornilov (2015) data might be accepted. Uncertainties for all experimental data were carefully quantified based on the literature and data in EXFOR. Small missing uncertainties were estimated with PFNS templates of expected uncertainties. We use IRLS (essentially what the standards call the “Chiba-Smith” algorithm) as evaluation technique which treats Peelle’s Pertinent Puzzle (PPP). Preliminary evaluation results show that there might be a bias in evaluated data because of PPP if this is not corrected for.

*Work at LANL was carried out under the auspices of the National Nuclear Security Administration (NNSA) of the U.S. Department of Energy (DOE) under contract 89233218CNA000001. This material is based upon work supported by the Department of Energy National Nuclear Security Administration through the Nuclear Science and Security Consortium under Award Number(s) DENA0003180 and the Office of Nuclear Physics under DE-20SSC000056 and DE-SC0021243. Work at Brookhaven National Laboratory was sponsored by the Office of Nuclear Physics, Office of Science of the U.S. Department of Energy under Contract No. DE-AC02-98CH10886 with Brookhaven Science Associates, LLC. The full summary report was approved by LANL for public release as LA-UR-25-21706.*

### 3.15. Bias identification in nuclear data measurements for experiment design, D. Neudecker (LANL, USA)

This talk is based on the work of Noah Walton as part of his internship at LANL for the AIACHNE team. This work focuses on applying machine learning techniques to explore unknown sources of uncertainties (coined USU as part of the standards). USU is a term that describes the systematic scatter across several datasets of which we do not understand the physics origin. Due to that, the standards decided to add uncertainties based on the spread of data. This procedure gives realistic evaluated uncertainties but leaves us in the dark as to the underlying physics drivers of the uncertainties. The AIACHNE project explores this by linking features describing the experiment set-up and analysis techniques with systematic biases evident in the data using a Bayesian model and a horseshoe prior. We apply this to  $^{252}\text{Cf}$  PFNS experimental data. The database was created as part of the AIACHNE effort to re-evaluate the  $^{252}\text{Cf}$  PFNS and features were extracted from the literature and EXFOR entries of each dataset. It was shown at the example of Boldeman  $^6\text{Li}$  data that the algorithm not only correctly identifies that there is a bias in the data from 200-400 keV but also links it correctly to using a  $^6\text{Li}$  detector. It also assesses the size of this bias. This combined information can help evaluators identify what are driving biases in experimental data and quantify the bias size for uncertainty quantification purposes. In this validation case, we knew that the bias stems from incorrect analysis of the  $^6\text{Li}$  detector response. However, a second example was shown with a bias at high outgoing neutron energies in several datasets. It was unclear which features could be realistically linked to bias. The ML algorithm would have linked it to the fission-fragment efficiency which encouraged experimenters and evaluators to further explore this feature and if it could lead to bias. In fact, it could be that there is an issue in the fission fragment efficiency in Maerten data as he measures at two angles with nearly the same set-up and the same analysis technique, Still, one sees systematic deviations between the two measurements that could be likely linked to fission-fragment angular distribution and insufficient treatment within the fission-fragment detector response function. In summary, a method was developed that explores the physics origin of systematic biases in data. The Bayesian model with a horseshoe prior allows us to link features of data with biases. In addition, it quantifies the energy range of the bias and its strength. This information can help experimenters and evaluators to further explore biases in data, then reject, correct data or enlarge uncertainties for the dataset in question-ultimately reducing the need to quantify uncertainties based on the spread of a database.

*Work at LANL was carried out under the auspices of the National Nuclear Security Administration (NNSA) of the U.S. Department of Energy (DOE) under contract 89233218CNA000001. This material is based upon work supported by the Department of Energy National Nuclear Security Administration through the Nuclear Science*

and Security Consortium under Award Number(s) DENA0003180 and the Office of Nuclear Physics under DE-20SSC000056 and DE-SC0021243. Work at Brookhaven National Laboratory was sponsored by the Office of Nuclear Physics, Office of Science of the U.S. Department of Energy under Contract No. DE-AC02-98CH10886 with Brookhaven Science Associates, LLC. The full summary report was approved by LANL for public release as LA-UR-25-21706.

### 3.16. New experimental data for the GMAPy database update since 2017 evaluation, V.G. Pronyaev (private, Russia)

Since the last Neutron Data Standards release in 2017 (referred to as Standards2017), more than 20 new datasets can be retrieved from EXFOR and included in the GMAPy database. Datasets obtained at the same installations (nTOF, NIFFTE TPC, CSNS Back-n) have components of uncertainties with strong correlations which should be taken into account. The improvement of the standards can be expected in the fission cross sections, capture cross sections below 100 keV and in R-matrix evaluation for light element standards.

The Table with references at the source of data and figures illustrating their consistency/discrepancies with Standards2017 evaluation are given.

#### CSNS Back-n measurements for light elements standards

A new analysis of the ratio of boron alpha emission reactions to  ${}^6\text{Li}(n,t)$  was done by Liu (2023). It is based on two separate results of measurements by Bai for  ${}^6\text{Li}(n,t)$  ( $X4=32800$ , 2020) and by Jiang for  ${}^{10}\text{B}(n,\alpha_0)$ ,  ${}^{10}\text{B}(n,\alpha_1)$  and  ${}^{10}\text{B}(n,\alpha)$  ( $X4=32804$ , 2019). This was possible because the  ${}^{235}\text{U}(n,f)$  cross section was used in these two separate measurements for flux determination and it can be excluded in the ratio. The Liu ratio of the  ${}^{10}\text{B}(n,\alpha)/{}^6\text{Li}(n,t)$  integral in the energy range 1 eV – 1 keV from the 2017 Standards ( $R=4.083$ ) was used for ratio normalization. Due to this, the status of the data type is the shape of ratio.

The calculated ratio Jiang  ${}^{10}\text{B}(n,\alpha)$  ( $X4=32804002$ ) to Bai  ${}^6\text{Li}(n,t)$  ( $X4=32800002$ ) is compared with the ratio obtained in the analysis by Liu, normalized to the ENDF/B-VIII. The difference between the Liu ratio normalized to Standards2017 and the ratio directly calculated from Jiang and Bai measurements is about 2%. The difference in the shape of the ratio near the 245 keV resonance in the  ${}^6\text{Li}(n,t)$  (Fig. 1) exceeds one standard deviation.

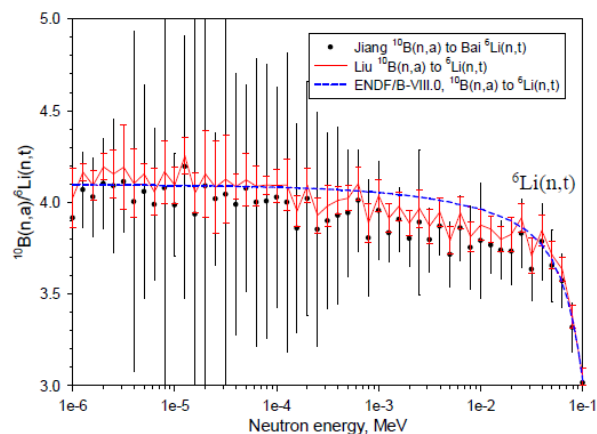


FIG. 1 Comparison of the CSNS Back-n measurements with Standards2017.

It is concluded that:

- the results of Liu  ${}^{10}\text{B}(n,\alpha)$  and  ${}^{10}\text{B}(n,\alpha_0)$  to the  $\text{Li}(n,t)$  ratio analysis can be used in the GMA fit as shape of ratio data. To avoid double counting, the ratio  ${}^{10}\text{B}(n,\alpha_1)/{}^6\text{Li}(n,t)$  should not be used in the fit.  ${}^{10}\text{B}(n,\alpha)$  is taken because it is presented up to 2.4 MeV.
- the partial uncertainties are not given at Liu ratios. The partial uncertainty for the ratio can be estimated from components of the uncertainties given for  ${}^6\text{Li}$  and  ${}^{10}\text{B}$  measurements.

Components of the uncertainties related to the flux and mass determination are not valid for shape of ratio data.

- the other problem is that the relative uncertainties given in Jiang (X4=32804) for  $^{10}\text{B}(n,\alpha)$ ,  $^{10}\text{B}(n,\alpha_0)$  and  $^{10}\text{B}(n,\alpha_1)$  for some components are identical, which is implausible from the physics point of view. Some points between 1 keV and 30 keV can be treated as outliers.
- relative angular distributions for  $^{10}\text{B}(n,\alpha_0)$ ,  $^{10}\text{B}(n,\alpha_1)$  and  $^6\text{Li}(n,t)$  could be used in the R-matrix fits.

**nTOF experimental data (Mingrone 2017) for  $^{238}\text{U}(n,\gamma)$  reaction**

The reason for the discrepancy (Fig. 2) with the Standards2017 results above 70 keV is not clear. The Mingrone’s data above 70 keV should be excluded from the evaluation.

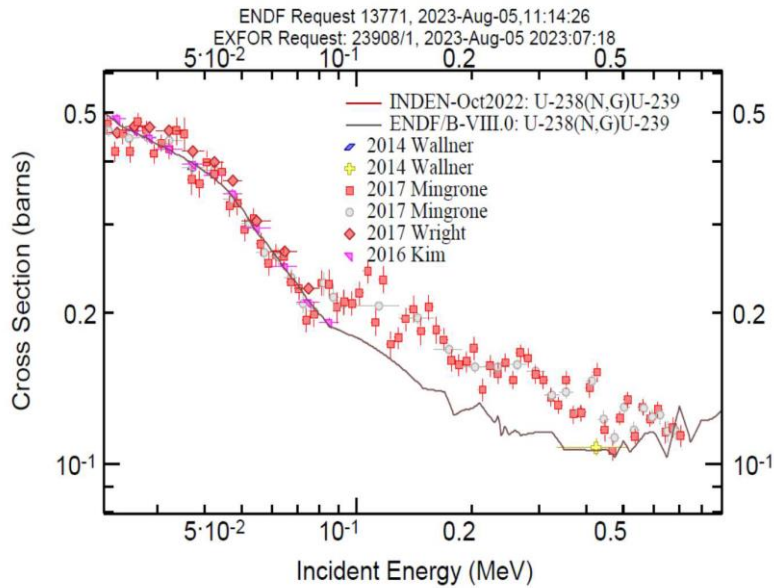


Fig. 2. Results of nTOF measurements (Mingrone 2017) in comparison with present evaluations

Excellent consistency is observed between nTOF measurements done with 2 different detectors below 70 keV: the C6D6 detector in the measurements by Mingrone and the BaF2 detector in the measurements by Wright (Fig. 3). They should be used in the Standards fit with correlation between common components of the uncertainties.

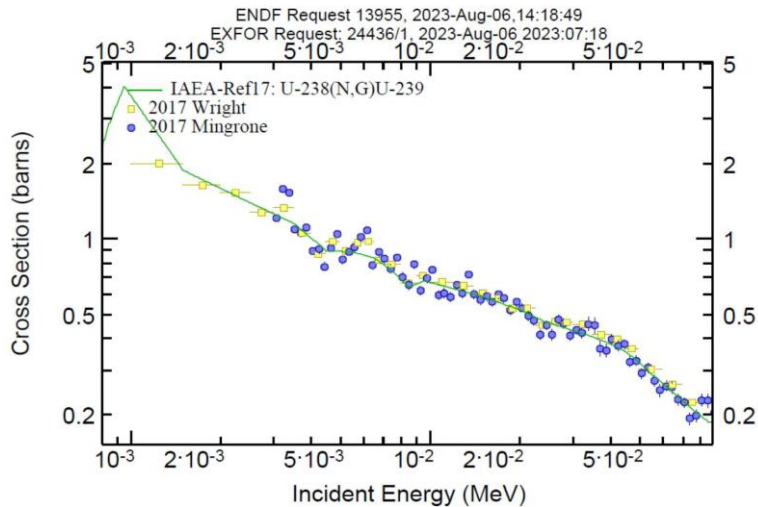


FIG. 3. nTOF measurements for  $^{238}\text{U}(n,\gamma)$  below 70 keV.

### CSNS Back-n capture cross section measurements for $^{197}\text{Au}$

The derived cross sections shown in Fig. 4a) are corrected for multiple scattering and background. However, the multiple scattering correction used in the resonance range is smooth. It should be resonance dependent and could be obtained from resonance capture area measurements done only with an MC simulation. Average cross sections in Fig. 4b) are 20-30% higher than Standards2017 in the URR.

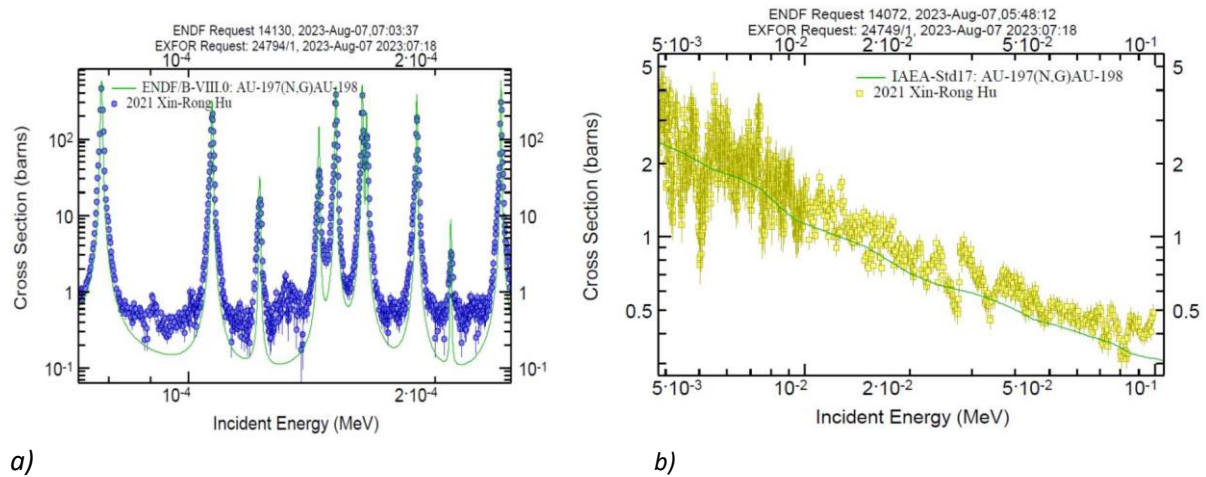


FIG. 4. Results of CSNS Back-n capture cross section measurements for  $^{197}\text{Au}(n,\gamma)$  in comparison with evaluated data: a) in the resolved resonance range, b) in the unresolved resonance range.

Data cannot be used in the Standards evaluation.

### ANNRI beam line $^{197}\text{Au}(n,\gamma)$ cross section measurements (Rovira, 2021)

The accelerator pulsed double bunch mode was used to increase statistics and obtain results with a statistical uncertainty of 1%. This led to a double peaked wide resolution pulse. Data (Fig. 5) can be used in GMAPy as SACS data. The spectra are available at: <https://wwwnds.iaea.org/exfor/servlet/X4sGetSubent?plus=1&sub=23746003,23746004,...23746005>.

### Activation $^{197}\text{Au}(n,\gamma)$ measurements by Vansola

Data by Vansola (Fig 5) cannot be used in the Standards, because the  $^{115}\text{In}(n,\gamma)^{116\text{m}}\text{In}$  reaction was used as the monitor reaction in the measurement.

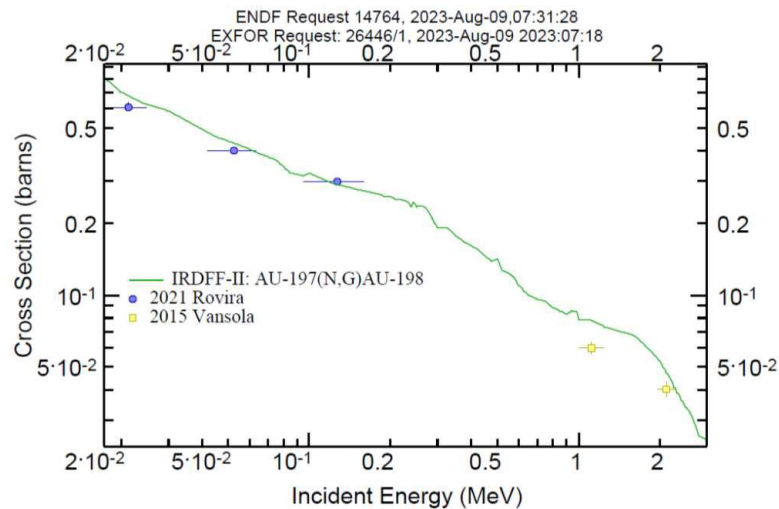


FIG. 5. Comparison of the Standards2017 evaluation (accepted by IRDFF-II) with the results of ANNRI measurements and Vansola activation measurements.

### nTOF fission cross section measurements

The nTOF measurements of  $^{235}\text{U}(n,f)$  by Amaducci(2019) were done relative to  $^6\text{Li}(n,t)$  and  $^{10}\text{B}(n,\alpha)$  in the same neutron beam run. The ratios were normalized using Standards (2017) ratios of  $^{235}\text{U}(n,f)/^6\text{Li}(n,t)$  and  $^{235}\text{U}(n,f)/^{10}\text{B}(n,\alpha)$  in the energy range 7.8 eV – 11 eV. Because of this, they can only be used as shape of ratio measurements. A visible difference with Standards (2017) was observed at 9, 15 and above 70 keV.

The irregularities of non-statistical nature can be clearly seen at 9 and 15 keV in the reconstructed ratio of  $^{10}\text{B}(n,\alpha)/^6\text{Li}(n,t)$  cross sections (Fig. 6), which should be smooth.

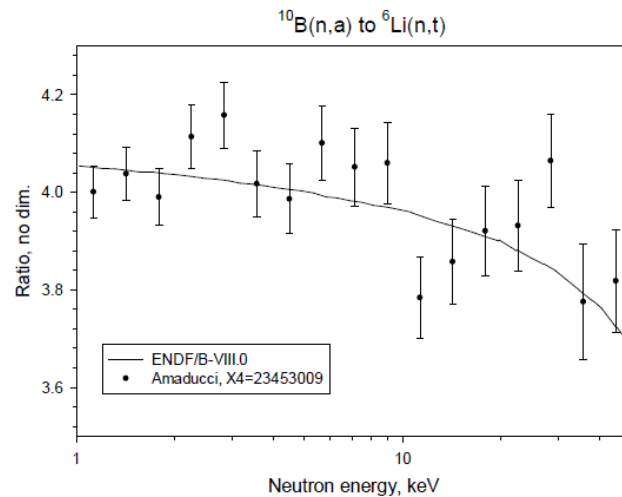


FIG. 6.  $^{10}\text{B}(n,\alpha)/^6\text{Li}(n,t)$  ratio derived from nTOF measurements in comparison with Standard ratio.

It was also shown that results of many fission cross measurements, if reduced to the nodes used in the standards evaluation, do not support the energy dependence observed in the nTOF measurements reduced to the same nodes in the energy range 8 – 20 keV.

### NIFFTE TPC LANL fission cross section ratio measurements

The results of  $^{238}\text{U}(n,f)/^{235}\text{U}(n,f)$  (2018) and  $^{239}\text{Pu}(n,f)/^{235}\text{U}(n,f)$  (2021) ratio cross section measurements can be used as shape data because of their normalization at the standards. Uncertainties and correlation matrices were prepared by performing a complete error propagation analysis and are given in EXFOR entries X4=14721 and X4=14756. They will substantially improve the cross sections above 20 MeV. The results of the latest measurements  $^{238}\text{U}(n,f)/^{235}\text{U}(n,f)$  by TOF technique (LANL – Casperson, PNPI – Vorobyev and CSNS - Zhizhou Ren and Jie Wen) are very consistent.

### nTOF fission cross section measurements

The results of  $^{238}\text{U}(n,f)/^{235}\text{U}(n,f)$  absolute cross section ratio measurements by Paradela (2016) in the wide energy range include 7 correlated datasets (Fig. 7). They should replace preliminary data used in Standards2017 evaluation.

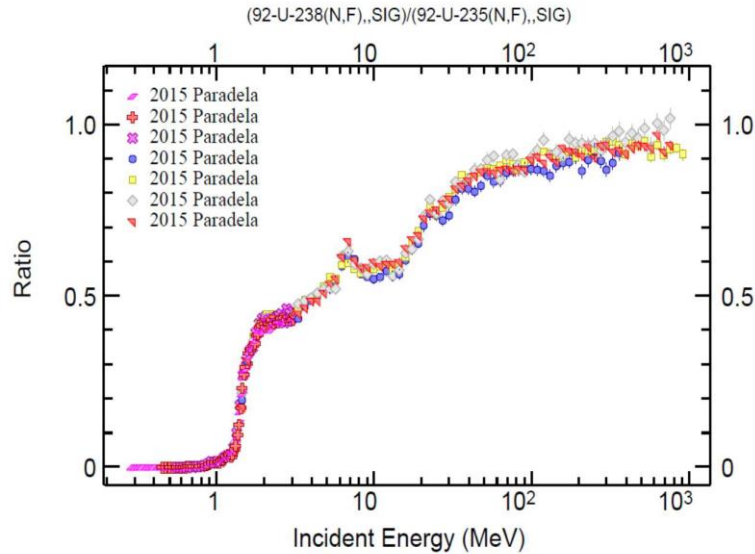


FIG. 7. Results of  $n\text{TOF } ^{238}\text{U}(n,f)/^{235}\text{U}(n,f)$  ratio measurements done with different detectors and measurement conditions.

The data spread (up to 5% at high energy) demonstrates the systematic uncertainties due to variation of the measurement conditions.

#### PNPI fission cross section measurements

The results of the TOF  $^{238}\text{U}(n,f)/^{235}\text{U}(n,f)$  measurements by Vorobiev are in good consistency with the Standards2017 evaluation below 200 MeV. Above 200 MeV there can be a difference of 5% to the present Standards ratio. All components of the uncertainties are given and should be used for constructing the covariance matrix in the GMA fit.

#### CSNS fission cross section measurements

The first dataset is the result of absolute ratio measurements  $^{238}\text{U}(n,f)/^{235}\text{U}(n,f)$  by Zhizhou Ren (2023) in the energy range 0.5 -175 MeV with an uncertainty of 1.5% in the determination of the ratio of the sample masses. The second dataset by Jie Wen (2018) presents the absolute ratio measured in the energy range 1 – 20 MeV. Some components of the uncertainties are strongly correlated between these two datasets. There is good consistency with the Standards2017 evaluation and other experimental data in the same energy range. The total uncertainty is below 3% in the energy range between 1.5 and 150 MeV. Both datasets should be included in the Standards database.

#### PTB-GEEL absolute fission cross section measurements

The Belloni (2022) absolute measurements at 2.51 and 14.83 MeV are done relative the PTB hydrogen long counter used as German primary standard for neutron flux measurements. Results for two fission chambers (Fig. 8) are differ by 2% at 2.51 MeV and by 5% at 14.53 MeV. There are common components of the uncertainties and correlated components of the uncertainties for 4 experimental values with 2 chambers at 2 energies.

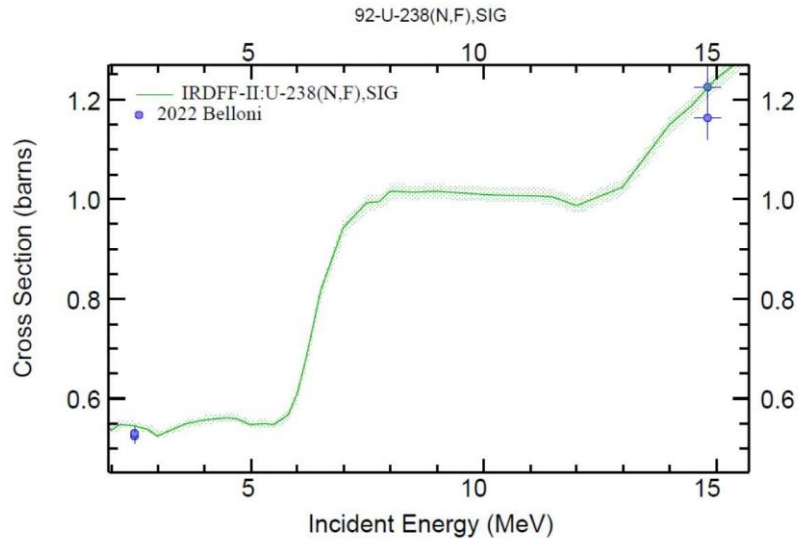


FIG. 8 Comparison of the results of absolute  $^{238}\text{U}(n,f)$  cross section measured in PTB with the Standards2017 evaluation.

Two identical fission chambers with slightly different loads of  $^{238}\text{U}$  give a 2% difference at 2.51 MeV and 5% at 14.53 MeV in the determined fission cross section. This shows that at least some part of the differences is not related to the uncertainties in the mass of the  $^{238}\text{U}$  samples. The publication does not provide enough details, especially on how the angular anisotropy of fission fragment yields is accounted for, to allow for definitive conclusions. The data should be included in the Standards database.

New experimental data obtained since the Standards2017 evaluation and still not included in the GMA database may contribute to the improvement of the evaluation even if they are consistent with the Standards2017 evaluation.

### 3.17. Evaluations for $^1\text{H}$ , $^3\text{He}(n,p)$ , $^7\text{Li}$ , $^{11}\text{B}$ , $^{13}\text{C}$ systems with RAC, Z. Chen (Tsinghua University, China)

Results of an R-matrix evaluation using the RAC code were presented and compared with the neutron data standards2017 and the ENDF/B-VII nuclear data library. This comparison led to the following observations:

- The n-p evaluation below 1 MeV agrees well with the neutron standards evaluation 2017 but above 1 MeV, the appearance of some structures should be further investigated.
- The  $^3\text{He}(n,p)$  evaluation agrees with the ENDF/B-VII evaluation.
- For the  $^7\text{Li}$  system (various direct and inverse reaction channels are included) the following statements can be made:
  - There is an excellent agreement with ENDF/B-VII for the total cross section.
  - For elastic channel, at lower energy, ENDF/B-VII seems to be too high compared to data and the presented evaluation.
  - $^6\text{Li}(n,t)$  shows good agreement with the neutron standards2017, with differences of about 2% in the wings of the resonance.
- For the  $^{11}\text{B}$  system (various direct and inverse reaction channels are included), it was observed that:
  - The total cross section is in good agreement with ENDF/B-VII.
  - The elastic channel in ENDF/B-VII is slightly overestimated in the low energy range.
  - $^{10}\text{B}(n,\alpha)$  differs by about -2% to +6% compared to the standards2017.

- There are differences for  $^{10}\text{B}(n,\alpha_0)$  above 10 MeV between the presented evaluation and the standards2017. No data are available to resolve the discrepancy.
- The evaluations for  $^{10}\text{B}(n,\alpha_1)$  are in good agreement.
- For the  $^{13}\text{C}$  system (various direct and inverse reaction channels are included), it was shown that:
  - The total  $^{12}\text{C}(n,\text{tot})$  and  $^{12}\text{C}(n,n)$  are in good agreement with the standards2017 whereas for the elastic cross sections differences ranging from -1% to +2% can be observed.
  - New data from Peking University are available for  $^{12}\text{C}(n,n+3\alpha)$  below 15 MeV.

It was also emphasized that RAC can play an active role in the preparation of the next version of the neutron data and it was suggested that RAC and EDA may share the same database for in the future consistency.

### 3.18. Recent light-element standards-related work at Los Alamos, G. Hale, M. Paris, H. Sasaki (LANL, USA)

We summarized recent R-matrix work at Los Alamos on N-N (n-p), n- $^3\text{He}$ , and n- $^{12}\text{C}$  scattering. We had just begun to extend the N-N analysis to energies above 100 MeV by fitting the n-p total cross section at energies up to 250 MeV. We find that extending the energy range above 100 MeV is challenging with an R-matrix parametrization, since levels that were in the background are now in the energy range of the data and cause local fluctuations in what should be smoothly varying amplitudes.

A new evaluation has been performed for n- $^3\text{He}$  scattering based on an analysis of experimental data by Drogg and Otuka [1], which is very similar at energies up to about 10 MeV to the  $^4\text{He}$  R-matrix analysis that was used for ENDF/B-VIII.0. No changes were made in the  $^3\text{He}(n,p)^3\text{H}$  cross section at energies below 200 keV (it is a standard up to 50 keV). Angular distributions from the combined R matrix, Drogg-Otuka analysis were added for the reactions  $^3\text{He}(n,p)^3\text{H}$ ,  $^3\text{He}(n,d)^2\text{H}$  and  $^3\text{He}(n,\gamma)^4\text{He}$  at neutron energies up to 20 MeV.

New data were added to the n+ $^{12}\text{C}(^{13}\text{C})$  system analysis. The elastic and inelastic n+ $^{12}\text{C}$  angular distributions of Ramirez et al. [2] support the present analysis, and new inelastic data from the CoGNAC detector system are well described except in the region of a  $7/2^-$  resonance around 6.3 MeV. We are continuing efforts to resolve that difference, and to add new data above the  $\alpha+^9\text{Be}$  threshold. The normalization of some of the total cross-section data [3] has come down slightly in the region below 1 MeV, in better agreement with the experimental value.

We also are continuing our work on the n+ $^6\text{Li}$  ( $^7\text{Li}$ ) system analysis up to 8 MeV neutron energy in the hope of better characterizing the behavior of broad resonances evident in the  $^6\text{Li}(n,t)^4\text{He}$  cross section in the several-MeV region, which makes extending the present range of the standard above 1 MeV difficult.

No new work has yet begun on reactions in the n+ $^{10}\text{B}$  ( $^{11}\text{B}$ ) system, although many new measurements have been made since the last standards evaluation. We expect that analysis will be quite time-consuming to extend to higher energies as the number of excited-state  $^{10}\text{B}^*$  channels grows rapidly with increasing energy.

#### References:

- [1] M. Drogg and N. Otuka, Evaluation of the Absolute Angle-Dependent Differential Neutron Production Cross Sections by the Reactions  $^3\text{H}(p,n)^3\text{He}$ ,  $^1\text{H}(t,n)^3\text{He}$ ,  $^2\text{H}(d,n)^3\text{He}$ ,  $^3\text{H}(d,n)^4\text{He}$  and  $^2\text{H}(t,n)^4\text{He}$  and of the Cross Sections of Their Time-Reversed Counterparts up to 30 MeV and Beyond, Report INDC(AUS)-0019, January 2015.

- [2] A.P.D. Ramirez, E.E. Peters, J.R. Vanhoy, et al., Neutron elastic and inelastic scattering differential cross sections on carbon, Nucl. Phys. A **1023** (2022) 122446.
- [3] Y. Danon, et al., Beryllium and Graphite High-Accuracy Total Cross-Section Measurements in the Energy Range from 24 to 900 keV, Nucl. Sci. Eng. **161** (2009) 321.

## 4. REVIEW OF RECOMMENDATIONS AND ACTIONS OF PREVIOUS MEETING

- Data for absolute fission cross section measurement in the GMA database, performed at TUD/KRI and available in JENDL-5.0 selection are consistent.
- The absolute  $^{239}\text{Pu}(n,f)/^{235}\text{U}(n,f)$  data have been reviewed by D. Neudecker and the Standards Committee, and some of them converted to shape data.
- PFNS( $^{252}\text{Cf}$ ) datasets revisited by Denise.
- GLS and GPR comparison done for  $^{235}\text{U}(n,f)$ .
- Regarding the use of USU, several methodologies are proposed (comparison for simple test case, Bayesian USU methodology applied to full GMA database), a virtual meeting was held.
- Development to enable the inclusion of experimental covariance matrices in evaluations with AMUR code ongoing.
- Gmapy code development: Bayesian and MLE USU algorithm implemented; method for PFNS renormalization implemented; several spectra not implemented but easy to do if it is required; GMA database translated to JSON database accomplished.

## 5. RECOMMENDATIONS AND ACTIONS

### Recommendations and actions for Light elements

- LANL releases H evaluation up to 100 MeV (additional work ongoing to extend evaluation up to 250 MeV).
- Explore possibilities to provide an H evaluation up to 450 MeV based on experimental data.
- Provide a recommended cross section evaluation for H(n,g) at the thermal point.
- Recommend a new measurement of H(n,g) cross section at or below the thermal point.
- Adopt an extended  $^3\text{He}(n,p)$  cross section evaluation as combination of LANL and Drogg evaluation without changing the energy limit of the standards range.
- Explore the possibility to include the H evaluation for the purpose of automatic renormalization of all datasets measured relative to it with gmapy.
- Z. Chen and LANL: provide updated R-matrix evaluations of  $^6\text{Li}(n,t)$ ,  $^{10}\text{B}(n,\alpha)$ .
- IAEA to compare posterior uncertainties of R-matrix evaluations.
- New LANL evaluation for C to be released (ongoing).
- Release the data from JRC Geel for Cnat relative to  $^{235}\text{U}$ .
- Check if covariance matrices of  $^6\text{Li}(n,t)$  and  $^{10}\text{B}(n,\alpha)$  available in STD2017 database and in the newest database are the same (apart from USU).

### Recommendation and actions for $^{197}\text{Au}(n,\gamma)$

- Explore the possibility to consider  $^{197}\text{Au}(n,\gamma)$  SACS measurement in different spectra within the gmapy code/database (especially 25 keV and filtered neutron beams with known spectra, e.g. at RPI and ANNRI).

### Recommendation and actions for PFNS

- D. Neudecker: deliver PFNS( $^{252}\text{Cf}$ ) evaluation.

- D. Neudecker: provide experimental PFNS( $^{252}\text{Cf}$ ) data in order to reproduce their evaluation using Gmapy.

#### Recommendation and actions for Actinides

- R. Capote, D. Neudecker, A.D. Carlson: Because concerns about Cance data remain, review Cance absolute measurements (1976-1981) for actinides (check if data published 1978 in GMA database) (virtual meeting).
- Hold virtual meeting dedicated to USU methods and analysis.
- As soon as new experimental data become available (TPC ratios of  $^{235}\text{U}(n,f)/^6\text{Li}$  and  $^{239}\text{Pu}(n,f)/^{235}\text{U}(n,f)$ ; high energy  $^{235}\text{U}(n,f)/^1\text{H}$  data from A. Manna (nTOF) and from Y. Chen (CSNS Back-n), incorporate them into the GMA database.
- Incorporate the updates resulting from the analysis by V. Pronyaev into the GMA database.
- Incorporate the updates (i.e., changes from absolute to shape) of  $^{239}\text{Pu}(n,f)/^{235}\text{U}(n,f)$  data into the GMA database.
- Add a point at 235 keV for  $^{239}\text{Pu}$ .
- Make available GMA2017 fit by Simakov on the STD webpage ( $^{238}\text{U}$ ,  $^{235}\text{U}$  high-energy fission cross section).
- IAEA: Include the latest measurements Pb, Bi,  $^{239}\text{Pu}$ ,  $^{235}\text{U}$ ,  $^{238}\text{U}$  and repeat the high-energy evaluation up to 1 GeV.
- Consider different possibilities to deal with the discrepant datasets above 14 MeV up to 500 MeV for  $^{239}\text{Pu}(n,f)/^{235}\text{U}(n,f)$  and  $^{238}\text{U}(n,f)/^{235}\text{U}(n,f)$  and study the impact of different choices (e.g., rejection, USU, etc.) on the posterior values and uncertainties.
- Explore the reason for the large posterior difference between MCMC and MLE/GMAP for the  $^{235}\text{U}$ ,  $^{238}\text{U}$ ,  $^{239}\text{Pu}$  fission cross sections above 30 MeV (check the impact on USU).
- Use corrected JENDL-HE file (N. Otsuka can provide the corrected file for comparison, code used by JENDL: FISCAL (Fukahori)).
- Measurements of  $^{239}\text{Pu}(n,f)/^6\text{Li}(n,t)$  with the NIFFTE-TPC setup are encouraged and considered to provide valuable input to the standards project.

#### Recommendation and actions for SACS

- Review SACS  $^{235}\text{U}$ ,  $^{239}\text{Pu}$ ,  $^{238}\text{U}$  measurements in  $^{235}\text{U}(n_{\text{th}},f)$  PFNS and potentially add them to the GMA database.

#### Recommendation and actions for Code and Database

- Include documentation available in CRD file on experimental datasets in the GMA database.
- Include new experimental data in GMA database since STD2017 and exchange with experimentalists to clarify details.
- D. Neudecker: study impact of different scaling assumption on individual PFNS( $^{252}\text{Cf}$ ) experimental datasets.
- G. Noguere: provide input data for TNC including covariance matrices to G. Schnabel for an evaluation comparison between Axton, G. Noguere evaluation, GMA (also including I. Duran's work).
- Include I1 and I3 ratios to thermal points  $\sigma_a/I1$  and  $\sigma_a/I3$  for  $^{235}\text{U}$  and  $^{239}\text{Pu}$  as provided by I. Duran, fully correlated.
- Start with the re-evaluation of  $^{252}\text{Cf}(s.f.)$  nu-bar (especially UQ of Spencer and Smith data).

#### Recommendation and actions for USU

- G. Schnabel, LANL: Compare new methods and how to best merge them (biases, USU, etc.).

### **Suggestions for possible future work**

- A. Wallner: Follow up what  $^{239}\text{Pu}$  half live values was used in the past
- G. Noguere: Use R-matrix to calculate the integrals I1 and I3.
- All: Reflect whether I1 and I3 values should be provided as determined by G. Noguere and I. Duran or should they also be used in the evaluation with gmapy?

## APPENDIX I: ADOPTED AGENDA

### Monday 9 October (14:00 – 18:00, open 13:45 (all times Vienna time (GMT+2))

<b>14:00</b>	<b>Opening and Welcome address – Roberto Capote / Unit Head-NDDU</b>	
	<b>Introduction – G. Schnabel</b>	
	<b>Election of Chair and Rapporteur(s), Adoption of Agenda</b>	
<b>14:20</b>	<b>Participants' Presentations (~20'+10')</b> <i>Break as needed</i>	
A. Carlson	The Hydrogen Standard - The first and uniquely so	
G. Schnabel	Progress on the development of gmapy	
G. Noguere	Progress on the validation of the Thermal Neutron Constants	

### Tuesday 10 October (14:00 – 18:00)

<b>Participants' Presentations cont' (~20'+10')</b> <i>Break as needed</i>	
M. Anastasiou, L. Snyder	NIFFTE fissionTPC status update on $^{239}\text{Pu}(n,f)/^{235}\text{U}(n,f)$ and $^{235}\text{U}(n,f)/^6\text{Li}(n,f)$ cross section ratio measurements
I. Duran	New integral references for fissile actinides
J. Liu	Ratios of the cross sections for the $^{10}\text{B}(n,\alpha)^7\text{Li}$ reaction to the $^6\text{Li}(n,t)^4\text{He}$ reaction

### Wednesday 11 October (14:00 – 18:00)

<b>Participants' Presentations cont' (~20'+10')</b> <i>Break as needed</i>	
Y. Chen	Measurement of the fission cross-section of $^{235}\text{U}$ relative to n-p scattering from 10 to 70 MeV at CSNS Back-n
A. Manna	Absolute cross section of the $^{235}\text{U}(n,f)$ in the energy range between 20 and 450 MeV at CERN n_TOF
G. Noguere	Angular distribution measurements of neutron elastic scattering by natural carbon at GELINA with the ELISA setup
H. Iwamoto	A comparison of Gaussian process regression with GLS results for $^{235}\text{U}(n,f)$ cross section
D. Neudecker	Bias identification in Nuclear Data Measurements for Experiment Design

*Dinner at a restaurant (separate information)*

### Thursday 12 October (14:00 – 18:00)

<b>Participants' Presentations cont' (~20'+10')</b> <i>Break as needed</i>	
R. Capote	Impact and utility of SACS
D. Smith	Spectrum related SACS uncertainties
A. Wallner	U5 and U8 capture at subthermal
D. Neudecker	AIACHNE work towards a new $^{252}\text{Cf}(sf)$ PFNS evaluation
Z. Chen	Evaluations for $^7\text{Li}$ , $^{11}\text{B}$ , $^{13}\text{C}$ systems with RAC
G. Hale, M. Paris, H. Sasaki	Recent Light-Element Standards-Related Work at Los Alamos

### Friday 13 October (10:00 – 13:00)

10:00	Drafting of the Meeting summary report	<i>Break as needed</i>
13:00	Closing of the Meeting	

### Morning sessions (10:00 – 13:00)

#### Tuesday, 10 Oct (10:00 – 13:00)

$^{239}\text{Pu}(n,f)/^{235}\text{U}(n,f)$ : shape or absolute?

#### Wednesday, 11 Oct (09:30 – 13:00)

Experimental data, gmapy, validation & results

#### Thursday, 12 Oct (09:30 – 13:00)

Treatment of Unrecognized Sources of Uncertainty (USU) |

## APPENDIX II: PARTICIPANTS

Country	Name	Surname	Affiliation	Email	
<b>CHINA</b>		Yonghao	CHEN	Inst. Of High Energy Physics, CAS Spallation Neutron Source Science Center	chenyonghao@ihep.ac.cn
		Zhizhou	REN	China Academy of Engineering Physics, Inst. of Nucl. Physics & Chemistry	2248353512@qq.com
		Guohui	ZHANG	School of Physics, Peking University	guohuizhang@pku.edu.cn
		Jie	LIU	School of Physics, Peking University	1901110257@pku.edu.cn
<b>FRANCE</b>		Gilles	NOGUERE	Commissariat à l'énergie atomique et aux énergies alternatives	gilles.noguere@cea.fr
<b>GERMANY</b>		Anton	WALLNER	Helmholtz-Zentrum Dresden-Rossendorf	a.wallner@hzdr.de
		Ralf	NOLTE	Physikalisch-Technische Bundesanstalt	ralf.nolte@ptb.de
		Elisa	PIROVANO	Physikalisch-Technische Bundesanstalt	elisa.pirovano@ptb.de
<b>ITALY</b>		Alice	MANNA	Bologna University	alice.manna@bo.infn.it
<b>JAPAN</b>		Hiroki	IWAMOTO	Japan Atomic Energy Agency	iwamoto.hiroki@jaea.go.jp
<b>RUSSIA</b>		Sergei	BADIKOV	Rosatom State Corporation	legnitsa@mail.ru
		Vladimir	PRONYAEV	Private	vgpronyaev@yandex.ru
<b>SPAIN</b>		Ignacio	DURAN	Universidad de Santiago de Compostela	ignacio.duran@usc.es
<b>USA</b>		Allan	CARLSON	National Institute of Standards and Technology	carlson@nist.gov
		Denise	NEUDECKER	Los Alamos National Laboratory	dneudecker@lanl.gov
		Gerry	HALE	Los Alamos National Laboratory	ghale@lanl.gov
	 ?	Mark	PARIS	Los Alamos National Laboratory	mparis@lanl.gov
		Maria	ANASTASIOU	Lawrence Livermore National Laboratory	anastasiou2@llnl.gov

Country		Name	Surname	Affiliation	Email
USA cont'		Lucas	SNYDER	Lawrence Livermore National Laboratory	snyder35@llnl.gov
		Donald	SMITH	Private	donaldlarnedsmith@gmail.com
<b>INT. ORGANIZATION</b>		Carlos	PARADELA	European Commission, Joint Research Centre	carlos.paradela-dobarro@ec.europa.eu
		Georg	SCHNABEL	International Atomic Energy Agency	g.schnabel@iaea.org
		Roberto	CAPOTE	International Atomic Energy Agency	r.capotenoy@iaea.org
		Arjan	KONING	International Atomic Energy Agency	a.koning@iaea.org
		Naohiko	OTSUKA	International Atomic Energy Agency	n.otsuka@iaea.org



---

Nuclear Data Section  
International Atomic Energy Agency  
Vienna International Centre, P.O. Box 100  
A-1400 Vienna, Austria

E-mail: [nds.contact-point@iaea.org](mailto:nds.contact-point@iaea.org)  
Fax: (43-1) 26007  
Telephone: (43-1) 2600 21725  
Web: <https://nds.iaea.org>

---